

fibers to enhance its conductivity and solderability. Analytical evaluations and experimental mechanical and electrical characterizations have been conducted to conclude that the carbon fiber interconnect is a promising interconnect technique.

CARBON FIBER
ELECTRONIC INTERCONNECTS

By

Yuliang Deng

Dissertation submitted to the Faculty of the Graduate School of the
University of Maryland, College Park, in partial fulfillment
of the requirements for the degree of
Doctor of Philosophy
2007

Advisory Committee:

Professor Michael Pecht, Advisor and Chair
Professor Aris Christou
Associate Professor David Bigio
Professor Abhijit Dasgupta
Associate Professor Patrick McClusky
Professor Mohammad Al-Sheikhly

© Copyright by

Yuliang Deng

2007

Acknowledgements

I would like to thank my advisor, Professor Michael Pecht, for his guidance and support on my doctoral study all these three years. From him I learnt a lot, especially on how to conduct research in a high-quality and timely manner. It is a valuable experience working with him.

I would like to thank my supervisor, Dr. Ji Wu, who offered me uncountable help and guidance. I enjoyed the days when we were working together.

I would like to thank the rest of my dissertation committee members, Professor David Bigio, Professor Aris Christou, Professor Abhijit Dasgupta, Professor Patrick McClusky and Professor Mohammad Al-Sheikhly, for their time devoted on reviewing my dissertation, and attending my dissertation proposal and defense.

I would also like to thank all my colleagues in the CALCE center. It is an excellent experience of working with every one of you.

My best wishes to all of you.

Table of Contents

Acknowledgements.....	ii
Table of Contents	iii
List of Tables	vi
List of Figures.....	vii
List of Figures.....	vii
Chapter 1 INTRODUCTION	1
1.1 Background of carbon fibers.....	1
1.1.1 Overview and history.....	1
1.1.2 Applications	2
1.1.3 Forms of carbon fibers	5
1.1.4 Metal coatings on carbon fiber	9
1.2 Research motivation.....	11
Chapter 2 LITERATURE RESEARCH.....	12
2.1 Contact behavior of carbon fiber composites	12
2.2 Metal Coating.....	13
2.3 High frequency performance	14
Chapter 3 CARBON FIBER ELECTRONIC INTERCONNECT.....	15
3.1 Design concept.....	15
3.2 Parameters.....	18
Chapter 4 PRELIMINARY CHARACTERIZATIONS ON CARBON FIBER.....	20
4.1 Electrical characterization.....	20
4.1.1 Parasitic parameters	20
4.1.2 Experimental impedance analysis.....	20
4.1.3 Electrical resistance calculation.....	24

4.1.4	Self-inductance calculation	25
4.1.5	Skin effect analysis	27
4.1.6	Conclusions.....	28
4.2	Solderability investigation	30
4.2.1	Solder joint strength evaluation	33
Chapter 5	PROTOTYPES	36
5.1	Overview	36
5.2	Contact design.....	39
5.2.1	Contact resistance	39
5.2.2	Design for contact wipe	40
5.3	Insulating sleeve and carrier	42
5.4	Fabrication process	43
5.4.1	Contact preparation.....	43
5.4.2	Molding.....	43
5.4.3	Trimming and slicing.....	45
5.4.4	Contact surface preparation	45
5.4.5	Ultrasonic cleaning	46
5.5	Automated manufacturing process – water-jet cutting	46
Chapter 6	PROTOTYPE CHARACTERIZATION.....	48
6.1	Mechanical characterization	48
6.1.1	Force-deflection relationship	48
6.1.2	Cyclic loading test.....	53
6.1.3	Shear deformation due to CTE mismatch.....	57
6.2	Electrical resistance characterization.....	61
Chapter 7	SUMMARIES.....	65
7.1	Advantages.....	65
7.2	Limitations	65
Chapter 8	CONTRIBUTIONS	67

Chapter 9	SUGGESTIONS FOR FUTURE WORKS	68
9.1	Capacitance Characterization.....	68
9.2	Quantitative characterization of mechanical deflection.....	68
Appendices I	– Examples of LGA sockets	69
Appendices II	- Related U.S. Patents of electronics connectors.....	70
References	71

List of Tables

Table 1: Examples of electrical and electronics applications of carbon fiber	3
Table 2: Constant parameters in this research	19
Table 3: Analytical estimation of electrical resistance of carbon fiber	25
Table 4: Results of solder wetting test	31

List of Figures

Figure 1: A carbon fiber under scanning electron microscopy (SEM).....	1
Figure 2: Illustration of the microstructure of a PAN-based carbon fiber [1]	2
Figure 3: Carbon fibers in different one-dimensional continuous forms.....	6
Figure 4: Pultrusion process of carbon fiber composite [12].....	7
Figure 5: Cross section of a carbon fiber composite rod (1,000 filaments).....	8
Figure 6: Cross section of nickel-coated carbon fibers.....	10
Figure 7: Carbon fiber grid-array interconnect design	16
Figure 8: Permanent and separable contact	17
Figure 9: Schematic of test board for carbon fiber characterization.....	21
Figure 10: Resistance and reactance of individual plain carbon fiber	22
Figure 11: Resistance and reactance of individual nickel-coated carbon fiber	23
Figure 12: Inductance of bare carbon fiber and nickel coated carbon fiber	27
Figure 13: Skin depth versus frequency for different conductor materials	28
Figure 14: A fixture holding carbon fiber sample and copper substrate.....	32
Figure 15: A carbon fiber solder joint.....	32
Figure 16: Cross section of a carbon fiber solder joint.....	33
Figure 17: Test fixture for the tension test.....	34
Figure 18: Broken solder joint after the tension test.....	35
Figure 19: Prototypes of grid-array carbon fiber electronic interconnect devices.....	38
Figure 20: A carbon fiber composite rod with a brush at the end.....	40
Figure 21: A carbon fiber brush being compressed by a piece of glass	41
Figure 22: Close-up of a carbon fiber brush being compressed by a piece of glass.....	41
Figure 23: Mold for the fabrication of carbon fiber socket prototype	44
Figure 24: Raw contacts in the mold	44
Figure 25: Cross-section illustration of the mold in encapsulation	45
Figure 26: Surface processed by water-jet cutting.....	47
Figure 27: Test probe and contact under test	49
Figure 28: Force-Deflection Result - All Samples	50
Figure 29: Force-Deflection Result - Samples A and B	51
Figure 30: A cycle consisting of loading and unloading indicates an energy loss	52

Figure 31: Force-deflection result - Sample E.....	53
Figure 32: Probes and prototype under test	54
Figure 33: Loading profile	54
Figure 34: Force-deflection result of first 5 cycles.....	55
Figure 35: Microstructure of a contact before the cyclic loading test	56
Figure 36: Microstructure of a contact after the cyclic loading test	57
Figure 37: A schematic top view of a $N \times N$ array interconnect.....	58
Figure 38: A schematic cross-section view along the center and one corner contact.....	59
Figure 39: Pads offset due to CTE mismatch does not affect the contact integrity in this case.....	60
Figure 40: Test fixture for resistance characterization of the prototype.....	62
Figure 41: Diagram of the test circuit.....	62
Figure 42: Resistance-load characterization result (raw).....	63
Figure 43: Resistance-load characterization result (averaged, log-log).....	64

Chapter 1 INTRODUCTION

1.1 Background of carbon fibers

1.1.1 Overview and history

Carbon fiber is a synthetic fiber which has a micro graphite crystal structure. It typically has a diameter of few microns. It is made by a high temperature treatment process from a precursor fiber material. Common precursor fiber materials include polyacrylonitrile (PAN), rayon and pitch [1]. Thus, typical carbon fiber can be grouped into three types: PAN-based, pitch-based, and rayon-based. [1].

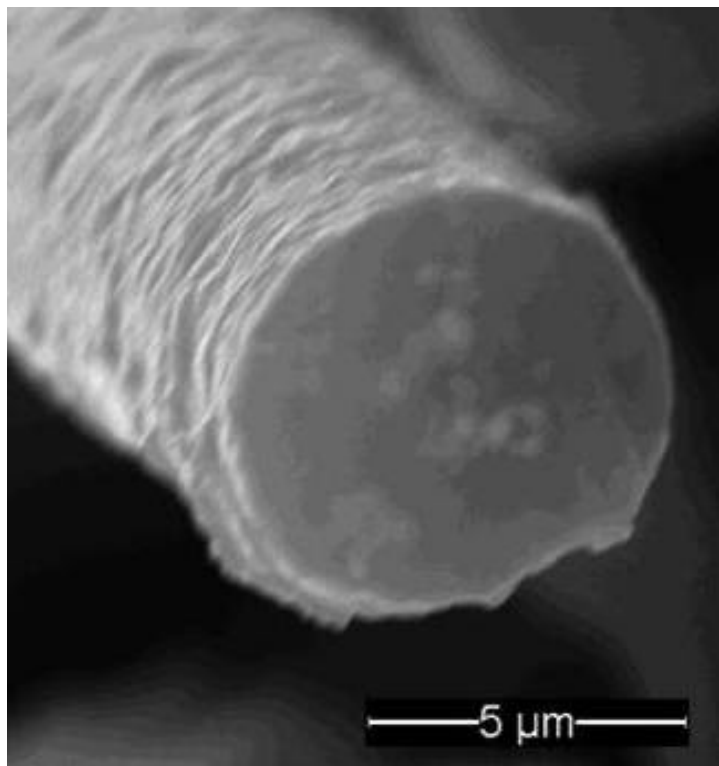


Figure 1: A carbon fiber under scanning electron microscopy (SEM)

Industrial production of carbon fibers started with rayon-based carbon fiber since 1950's. In 1960's, the methods of making carbon fiber from PAN and pitch were developed. There are two types of pitch based carbon fiber: isotropic pitch fibers which

has low mechanical properties and relatively low cost, and mesophase pitch fiber which has very high modulus. Nowadays, PAN-based carbon fiber takes the largest fraction of the carbon fiber industry, which has high strength and modulus.[1] From a microstructural view, a carbon fiber can be considered as a roll of graphite layers, as shown in Figure 2 [1].

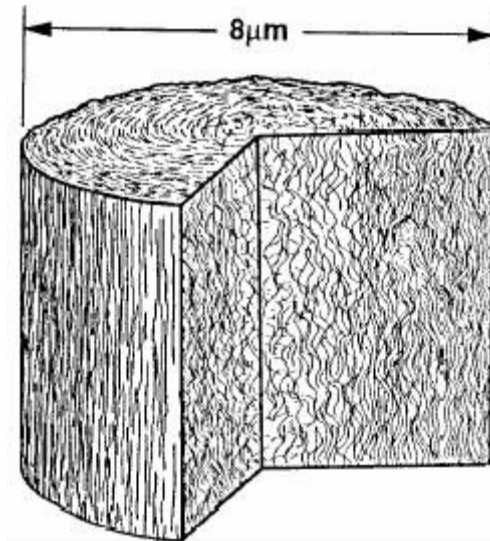


Figure 2: Illustration of the microstructure of a PAN-based carbon fiber [1]

1.1.2 Applications

The earliest recorded application of carbon fiber was in light bulbs. This was attempted by Joseph Swan in 1860's and then Thomas Edison in 1879 [2]. However, it is well known that tungsten was soon found to be an ideal material to make light bulb.

Carbon fiber has been used as structural materials for many years in a number of applications, such as aerospace, transportation (used in Boeing 787 Dreamliner, Airbus A350 [2]), sports equipments (e.g. race-car, golf club, tennis racket) and other consumer products (e.g. tripod). Carbon fiber is favored in these structural applications due to its

superior tensile strength and low specific weight, compared to traditional metal structural materials, such as structural steel and aluminum alloys¹.

In 1895, Elihu Thomson invented a commutator brush made of metal coated carbon fibers [4]. This was the first successful application of carbon fiber in electrical industry. Since recent few decades, carbon fiber materials have found more applications in electrical and electronics industry. Typical applications include brush contacts in 1) commutators [4][5], position sensors [6][7], switches [8][9], and static discharge eliminator devices [10][11][12]; 2) electrodes in capacitors [13], microwave tubes [14], and electrodes for brain research [15][16]; 3) electromagnetic interference shields [17]; 4) Audio cable [18][19][20][21]. Details are listed in Table 1.

Table 1: Examples of electrical and electronics applications of carbon fiber

	Applications	User / inventor / researcher, year and reference
Brush contact	Commutator brush	E. Thomson, 1895 [4], Y. Wu , 1995 [5]
	Position sensor (Potentiometer)	S. Liu, 2001 [6], R.F. Stinson, 2002 [7]
	Switches	Xerox Corp., since 1987 [8][9]
	Static discharge eliminator devices	Xerox Corp., since 1985 [10][11][12]
Electrode	Capacitors	S.M. Lipka, 1997 [13]
	Brain research	H.D. Manvelder, 1998 [15] J.G. Partridge, 2002 [16]
	Microwave tube	D.A. Shiffler, 2000 [14]

1 PAN based-carbon fiber, tensile strength: 3.5 - 4.7 GPa, density: 1.8 g/cm³[1]
 Aluminum alloys, tensile strength:, 0.3 - 0.5 GPa, density:2.7 g/cm³[3]
 Structural steel, tensile strength:, 0.3 - 1.7 GPa, density:7.8 g/cm³[3]

EMI shielding		D.D.L. Chung, 2001 [17]
Interconnect	Audio cable	<i>Van den Hul</i> , 1993 [18] [19][20], <i>Avantgarde</i> [21]

1.1.3 Forms of carbon fibers

Carbon fibers are usually used in multiple instead of individually, since single carbon fiber is brittle due to the fine size. Carbon fibers can be arranged as either continuous form or discrete (chopped) form. A group of continuous carbon fibers form bundles, sometimes known as yarn or tow, which is a One-dimensional form. Yarn can be woven to a two-dimensional laminar, or three-dimensional weaves. [1]

One-dimensional continuous carbon fibers can be arranged by themselves as carbon fiber bundle, or as carbon fiber composite, which is made by pultruding a bundle of continuous carbon fibers with a resin matrix. Carbon fiber bundles can be secured in a soft sleeve to prevent the carbon fibers from loosening and breaking. A carbon fiber bundle with sleeve appears to be, and in some case functions as, an electrical wire. Figure 3 shows few forms of carbon fiber, including carbon fiber bundle, carbon fiber composite rod and carbon fiber bundle in sleeve.

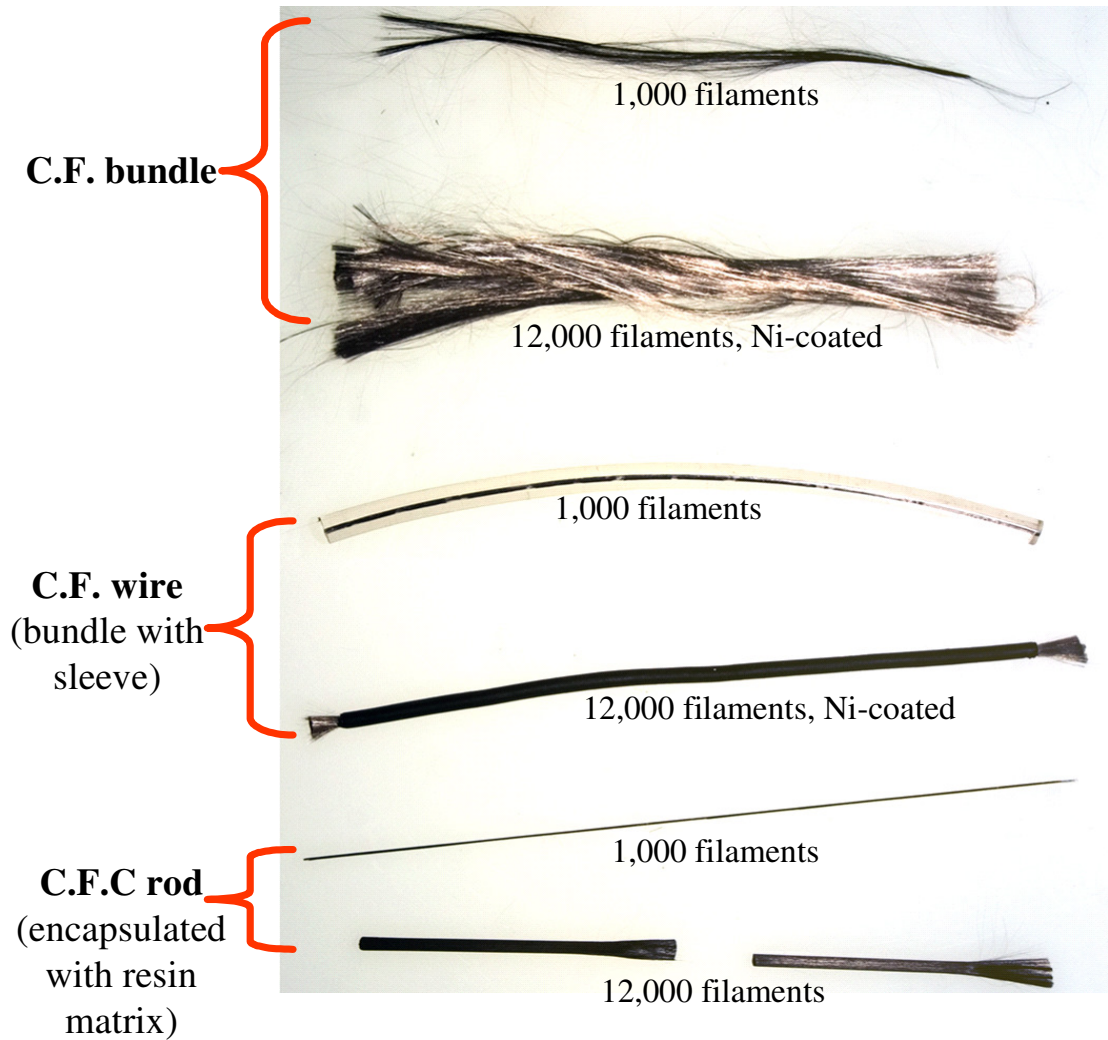


Figure 3: Carbon fibers in different one-dimensional continuous forms

Carbon fiber composites are made by pultruding bundles of continuous carbon fibers with a resin (e.g. cyanate ester). Figure 4 shows a typical pultrusion process for carbon fiber composites. Continuous carbon fibers are fed off creels and then move through a liquid resin impregnation bath in a resin tank. The carbon fibers are thereby coated with a crosslinkable polymer in the liquid phase. The wetted carbon fibers then pass through a forming/curing die where heat and pressure are applied to shape and cure

the components into a solid composite. Pullers, located in a region downstream of the die, provide force to move the composite through the various stages of the process. The cross sectional shape of the composite is determined by the shape of the die. For example, Figure 5 shows a cross section of a 0.3 mm diameter carbon fiber composite rod consisting of 1,000 carbon fibers. A carbon fiber tow or carbon fiber composite rod usually consists of a thousand parallel packed fibers or more.

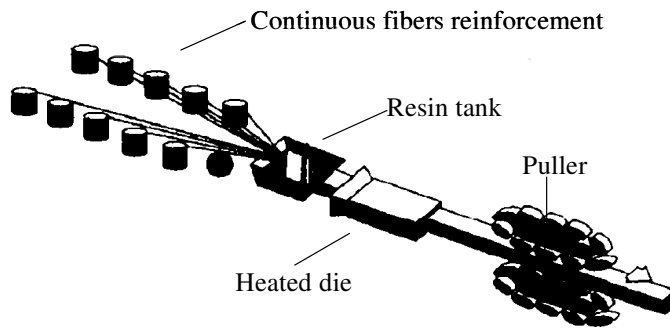


Figure 4: Pultrusion process of carbon fiber composite [12]

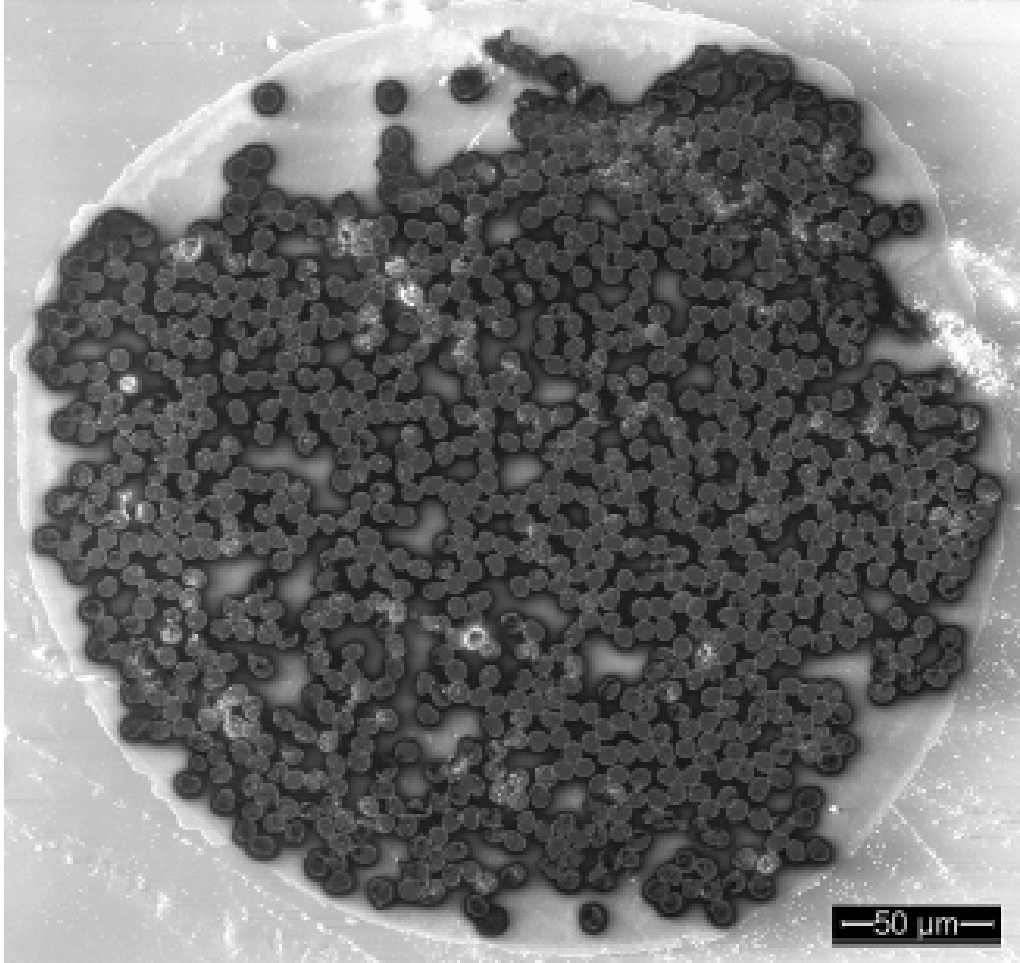


Figure 5: Cross section of a carbon fiber composite rod (1,000 filaments)

1.1.4 Metal coatings on carbon fiber

The electrical resistivity of carbon fiber is much higher than copper and aluminum which are usually used in electronics. For example, PAN-based carbon fiber has an axial resistivity of 9.5-18 $\mu\Omega\text{-m}$ [1], and the resistivity values of aluminum and copper are 0.027 $\mu\Omega\text{-m}$ and 0.017 $\mu\Omega\text{-m}$ [22]. In such a case, the difference is over one hundred times.

The effective resistivity can be lowered by coating carbon fiber with a metal layer. This idea was proposed as early as in 1895, when E. Thomson was developing the carbon (fiber commutator) brush [4]. Thomson suggested copper and nickel as candidate coating metals in his work [4]. The other candidate coating materials include aluminum [24] and zirconium pyronitride [25]. Figure 6 shows the cross section of a nickel coated carbon fiber.

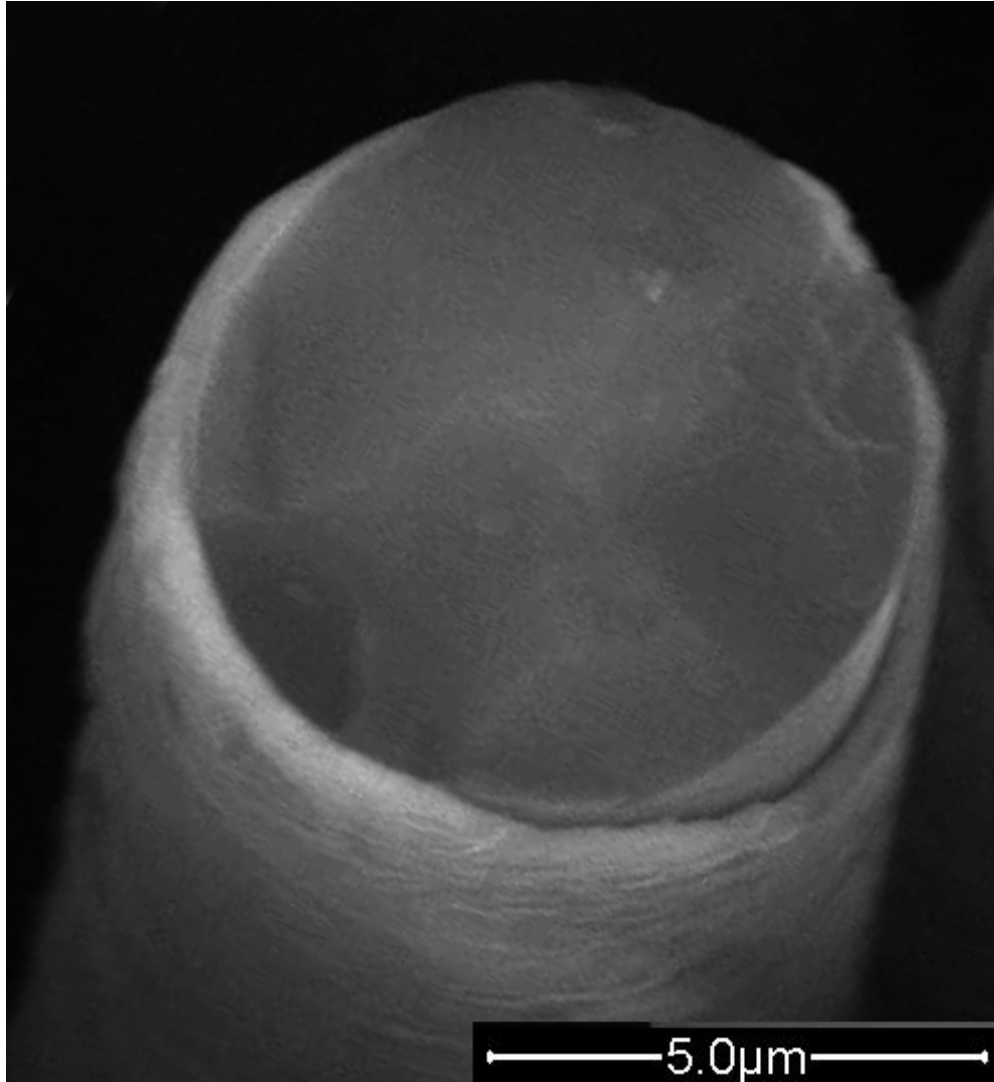


Figure 6: Cross section of nickel-coated carbon fibers

1.2 Research motivation

The objective of this dissertation is to carry out a research to see if it is possible to use carbon fibers to construct a grid-array inter-plane electronic interconnect device.

Carbon fiber is selected as the conductive medium, since it has shown some advantages in existing applications, which are believed to be able to contribute to the new proposed concept. These advantages includes contact redundancy[12][26][27][28], low contact wear [6][7], thermally and chemically stable [1], and environmental-friendly [20]. Some of these features will be elaborated in the following chapter: LITERATURE RESEARCH.

Chapter 2 LITERATURE RESEARCH

2.1 Contact behavior of carbon fiber composites

Carbon fiber materials, especially carbon fiber composites, have been used to construct brush contact in many applications. Their contact behaviors have been studied by many researchers, such as Wu [5] (1995), Swift and Wallace [12] (1997), Xie and Pecht [26][27] (1998-1999), Liu [6] (2001) and Stinson [7] (2002).

Wu [5], Liu [6] and Stinson [7] all observed a high stability of carbon fiber contacts in long term operation, in applications as potentiometer and commutator brush. From their researches, carbon fiber contacts were found to result low wear on the contact interface, compared to metal-to-metal contact pair [5][6][7]. The compliance of carbon fiber can reduce the energy loss and the wear between contact members, and thereby increase their operating life [6][7].

In some of these contact or interconnect applications mentioned above, a resistance of as large as in kilo-ohm range is considered acceptable [6][7]. However, in the carbon fiber electronic interconnect applications proposed in this study, the parasite electrical parameters of carbon fiber interconnect are critical to the system overall performance. In this application, a lower electrical bulk and contact resistance is highly desired, since such an electronic system is more sensible to the parasite parameters than high power electrical applications.

Swift and Wallace [12] attempted different contact surface preparation approaches on carbon fiber composites, in order to achieve a lower electrical contact resistance. The approaches included diamond cutoff wheel, laser, water-jet and flame. They discovered that a soft “fiber rich” contact surface tends to provide a lower electrical

contact resistance than a hard surface. Diamond cutoff wheel cutting leads to a hard surface without any free carbon fiber at the contact surface, and therefore results in a highest contact resistance among these approaches. Applying a flame to the surface can effectively remove the resin matrix near the surface and free the fibers in that region, and therefore results in a soft surface which leads to a low contact resistance. Xie and Pecht [26][27] developed a model to describe the contact resistance behavior of carbon fiber composite contacts.

In the proposed concept, short segments of carbon fiber bundles are used to construct the interconnect device. The previous researches on carbon fiber composites provide valuable references for this research. However, the electrical contact characteristics of carbon fiber bundles are not directly available from these previous studies. That is the reason why this research had to be conducted.

2.2 Metal Coating

As previously mentioned, resistance is a parameter to be minimized in an interconnect device. Metal coating is an efficient approach for that purpose. Common coating materials include nickel, copper and aluminum. C.T. Ho [23] compared nickel-coated carbon fiber and copper-coated carbon fiber in terms of mechanical properties in 1996. And they concluded that “nickel coating exhibited better bonding with the carbon fiber, compared to copper coating”; and composites with nickel-coated carbon fiber has higher tensile and shear strength than the ones with copper-coated carbon fibers [23]. In this research, nickel is used as the example for metal coating.

2.3 High frequency performance

Colloms [19] studied the performance of carbon fiber interconnect in high frequency, as in the application of audio cable. He concluded that carbon fiber is free from “skin effect”; its resistance remains frequency independent up to MHz range [19]. This behavior is a combined result of the small size of each filament conductor and the large number of parallel conductors. This feature may contribute to the proposed concept in this research. The skin effect of carbon fiber is evaluated and discussed later in the following chapter.

Chapter 3 CARBON FIBER ELECTRONIC INTERCONNECT

3.1 Design concept

A multiple I/O interconnect device is developed and evaluated in this research. The design concept is illustrated in Figure 7. The interconnect device consists of multiple carbon fiber bundles, each of which serves as a contact. The contacts are distributed as an array in a non-conductive carrier, which is also known as housing. The new device provides interconnect between two mating objects with planar surface. The mating objects can be a combination of semiconductor die, substrates, packaged components or printed circuit boards. The mating objects should have conductive pads in the same layout as that of the interconnecting device. For example, it can provide a separable interconnect between a land grid array (LGA) or ball grid array (BGA) IC package to a printed circuit board, as an LGA or BGA socket. In applications where the resistance is critical, metal-coated carbon fibers, e.g. nickel-coated, are recommended to construct the contact instead of plain carbon fibers.

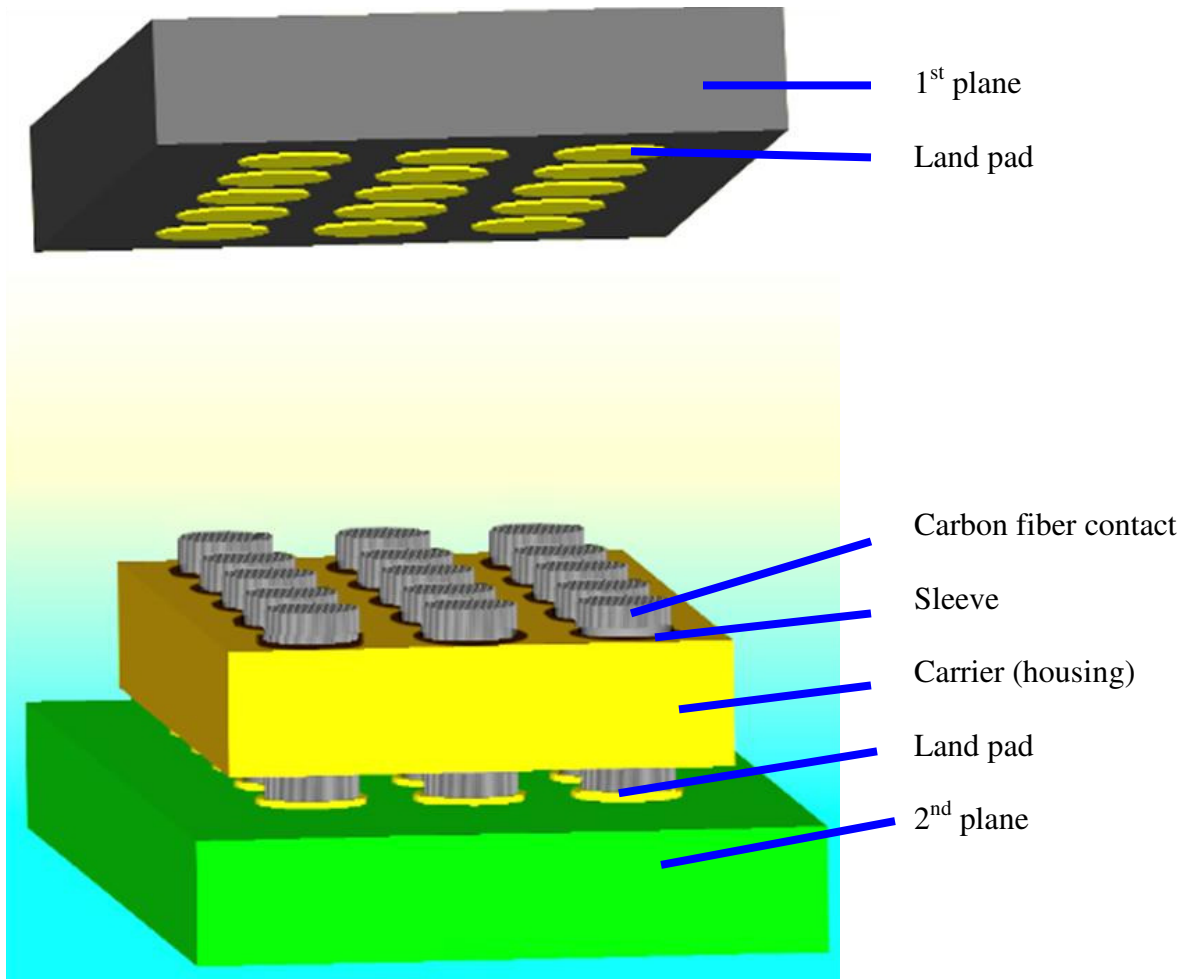


Figure 7: Carbon fiber grid-array interconnect design

Grid-array layout is selected since it is efficient to provide higher I/O density, over traditional in-line and peripheral interconnect layout. For example, for component-to-board interconnection, given a contact pitch of 1.27mm and package size of 42.5 mm², a grid array package can easily achieve over 1,000 I/Os, while QFP can only provide less than 200 I/Os [29].

The contact interface between the new interconnect to the mating objects can be either separable or permanent. In some cases, the interconnect device can be attached to one of the mating objects, e.g. printed circuit board, in a permanent manner, such as soldering. Each of them has its unique advantages: Separable contact enables easy field

replacement of a component package during a repair or upgrade; It enables multiple mating cycles, which is desired for product development, test and burn-in. Permanent contact can minimize contact resistance at the interface. For example, the resistance between a pad of an assembled BGA package and a board is typically below 1 m Ω , while it is tens of m Ω for LGA interconnection [34]-[36].

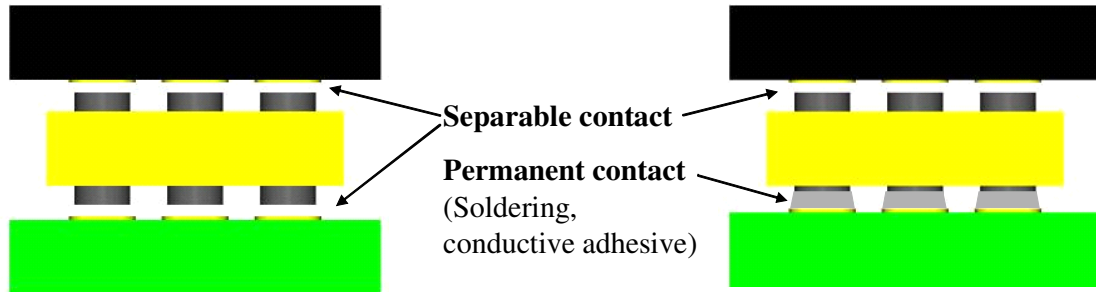


Figure 8: Permanent and separable contact

3.2 Experimental Procedures

Electric resistance, which is a sum of the bulk resistance of the contact and the contact resistance at the contact interface, is selected as the primary parameter to be optimized (minimized), because the primary function of this interconnect device is to conduct current. The electric resistance of a contact depends on the interconnect device design and the loading force in application.

There are many factors that can be varied in a design, including carbon fiber bundle length, carrier (housing) thickness, and loading conditions. The difference between the bundle length and the carrier thickness defines the height of the carbon fiber “brushes”, which determines the mechanical behavior of the contact when subjected to a normal force loading. In this research, the brush height is chosen to be the primary variable in a mechanical deflection study, which is varied in the range from approximately 0.5 mm to 1.2 mm, to evaluate its effects on the performance. Once an optimal height is identified, it will be used for the following electric resistance assessments.

In application, the loading force is preferred to be no more than 0.68 N (70g) on each contact pin. This is a typical range for most inter-plane grid-array separable interconnects in the market. For a high I/O count interconnect (e.g. > 1,000), the total contact force has to be limited to a degree that the board and IC assembly can sustain. In the preliminary mechanical characterization on individual contact pin, the force range is extended to 500% of the application limit (3.5N), in order to discover its behavior over a broader range.

The constant parameters in this research as listed in Table 2. Once the effects of current variable parameters are fully understood, some of these constant parameters can be varied in future study.

Table 2: Constant parameters in this research

Constant parameter	Value
Carbon fiber diameters	$7.5 \pm 1 \mu\text{m}$
Metal coating	1 μm nickel coating
Bundle size	12,000 filaments
Operating environment	Room ambient temperature and humidity
Carrier (housing) material in prototype	Epoxy

Chapter 4 PRELIMINARY CHARACTERIZATIONS ON CARBON FIBER

4.1 Electrical characterization

4.1.1 Parasitic parameters

The performance of an electronics system is determined by the combination of the electronic components as well as the interconnects between the components. There is movement in the electronics industry towards high speed, high power and high integration. These trends raise the requirement for interconnects as well as for components. Electrical resistance and self-inductance of the interconnects, together with capacitance and mutual inductance between interconnects represent critical factors in an electrical interconnect system. These factors are also known as parasitic parameters. Resistance is always a concern, especially for high power applications, because the resistance of an interconnect induces joule heat and related power loss during operation. Inductance and capacitance are critical for AC applications, especially for RF and microwave applications, because they may cause signal delay, distortion, and crosstalk. Resistance and self-inductance of PAN-based carbon fiber and nickel-coated PAN-based carbon fiber are studied in this section. The samples used in this study were manufactured by American Cyanamid Company. The product name of the nickel-coated fiber is CYCOM* NCG Fiber.

4.1.2 Experimental impedance analysis

Experimental impedance measurements were conducted on individual plain carbon fiber and nickel-coated carbon fiber. Two LCR (inductance/capacitance/

resistance) meters were used to measure the resistance and reactance over a frequency: Agilent 4263B LCR Meter for 100 ~ 100 KHz frequency range and Agilent E4285A Precision LCR for 75K ~ 30 MHz range.

A dedicated test board was designed and fabricated to attach the carbon fiber specimen (see Figure 9). On the top surface of the board, there are two gold plated copper strips as electrodes, spaced at 10 mm apart, which functioned as electrodes. Therefore when a carbon fiber specimen is attached to the electrodes, the effective measurement length is 10 mm. An electrically conductive adhesive, Silver Print from GC Electronics, was used to attach the fiber samples to the electrodes. The electrodes were connected to the LCR meter for measurement, using four-wire-connection method. Before the test on carbon fiber specimen, the LCR meter was calibrated and compensated with the test board attached, at an open, short and 50 Ω load condition.

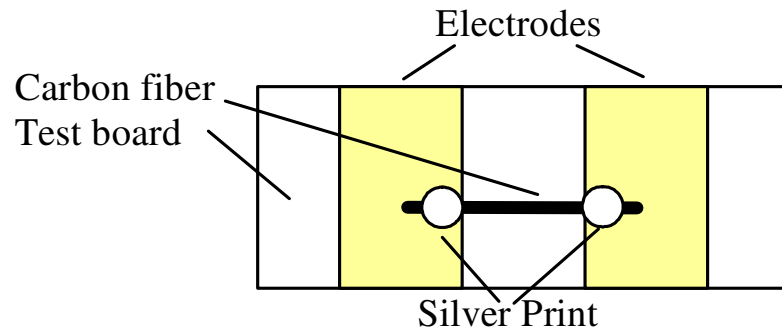


Figure 9: Schematic of test board for carbon fiber characterization

Three bare carbon fibers and three nickel coated carbon fibers were tested individually. The measured resistance and reactance results are plotted versus frequency in Figure 10 and Figure 11.

Carbon fiber and nickel coated carbon fiber show stable purely resistive behavior over the measurement frequency range from 100 Hz to 2 MHz. Reactance, which is

induced by inductance and capacitance, is negligible on this plot from the characterization. The test results will be compared with analytical calculated values, using parameters and formulas from literature, in the following sections.

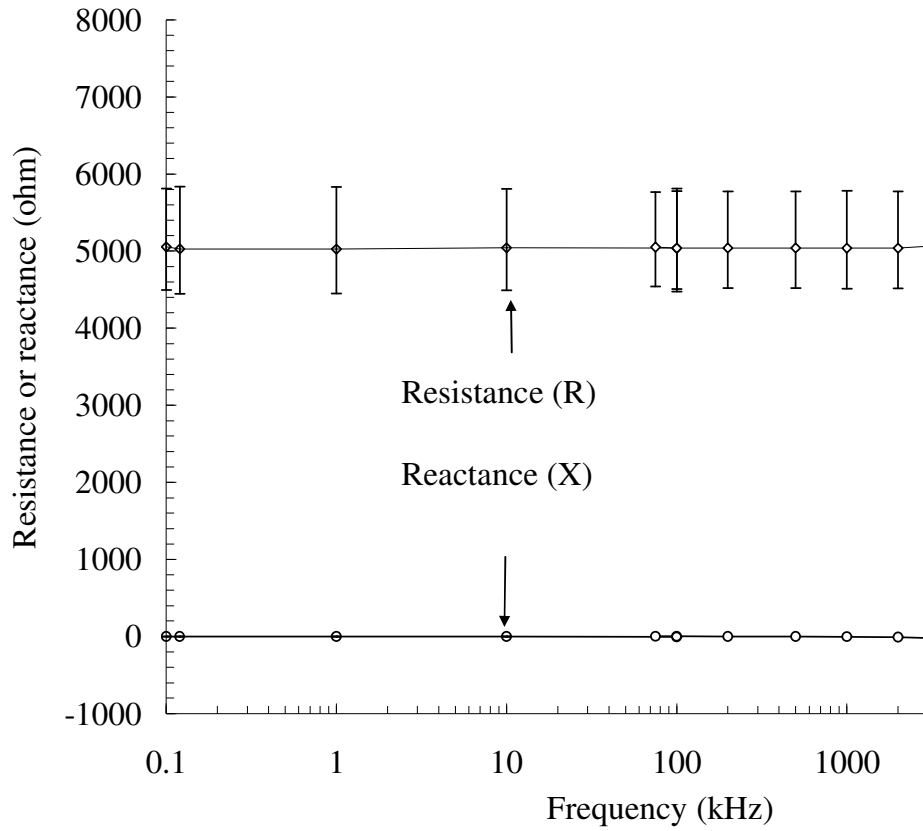


Figure 10: Resistance and reactance of individual plain carbon fiber

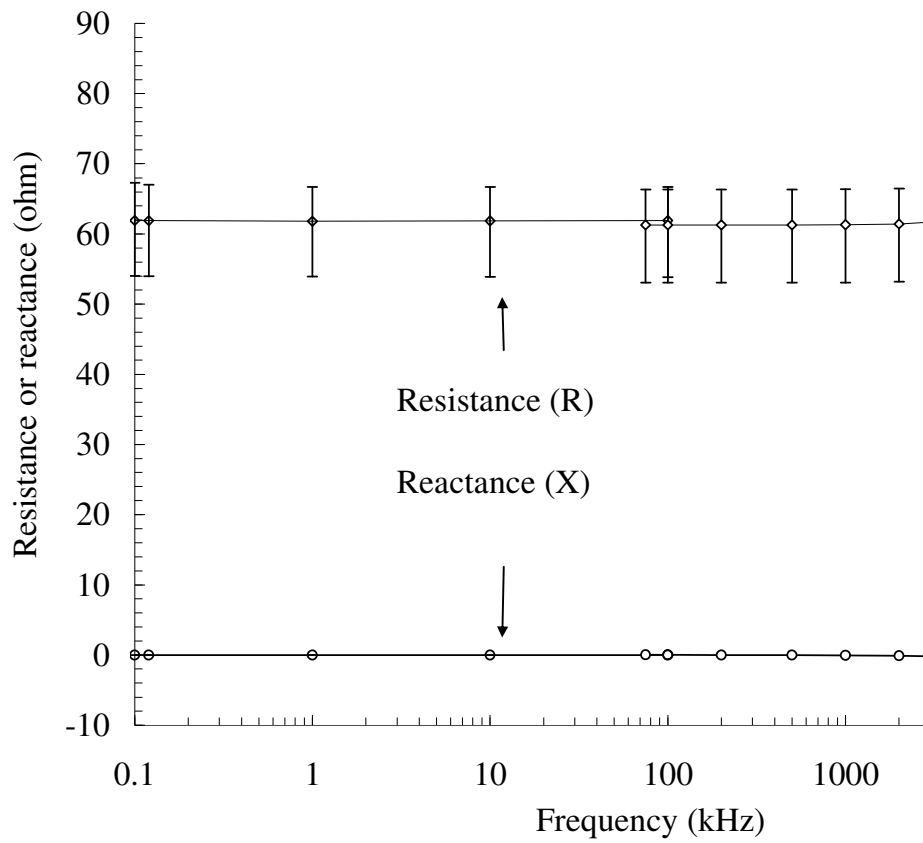


Figure 11: Resistance and reactance of individual nickel-coated carbon fiber

4.1.3 Electrical resistance calculation

Resistance of PAN-based carbon fiber and nickel-coated carbon fiber can be estimated using the material resistivity and geometry configurations. The values of resistance per unit length of individual carbon fiber and nickel coating are determined by the fundamental equation: $R = \frac{\rho \cdot l}{A}$, where the resistivity of PAN-based carbon fiber is 9.5-18 $\mu\Omega\text{-m}$ along its longitudinal axis [1] and the diameter of carbon fiber is 7 μm . The resistance of individual plain carbon fiber is directly calculated out to be 300-600 Ω resistance per mm.

For nickel-coated carbon fiber, since the resistivity of nickel (0.07 $\mu\Omega\text{-m}$) is two orders of magnitude smaller than that of carbon fiber, the current can be assumed flowing through the nickel coating only. The resistance of individual nickel-coated carbon fiber can be approximated as that of a nickel tube conductor. When the nickel coating is 1- μm thick, the resistance is calculated to be 6 Ω/mm . In such a case, carbon fiber serves as a mechanical support and medium, other than a primary conductor.

When thousands of carbon fibers are aligned in parallel to form a carbon fiber bundle or in carbon fiber composite, the total resistance is the parallel resistance of all

the fibers, namely $R_{total} = \frac{R_{individual}}{\text{Filament count}}$. Some example results are listed in Table

2. The experimental measured result of individual carbon fiber agrees with the theoretically calculated value.

Table 3: Analytical estimation of electrical resistance of carbon fiber

	Plain carbon fiber	Nickel-coated carbon fiber
Individual carbon fiber	300 - 600 Ω/mm	6 Ω/mm
Bundle or composite (1,000 filaments)	0.3 – 0.6 Ω/mm	6 m Ω/mm
Bundle or composite (10,000 filaments)	30 – 60 Ω/mm	0.6 m Ω/mm

4.1.4 Self-inductance calculation

For AC, inductance of a conductor can induce inductive reactance and cause a phase change of the signal. The self-inductance of a straight piece of carbon fiber can be calculated using the equation for a cylindrical non-magnetic conductor, Equation 1 [30].

$$L_{cylinder} = 2 \cdot l \left(\ln \left(\frac{2 \cdot l}{r} \right) - \frac{3}{4} \right) \cdot 10^{-7} \text{ (Henry)} \quad \text{Equation 1}$$

where $L_{cylinder}$ is the self-inductance of a non-magnetic cylinder, l and r are the length and radius of the conductor respectively. The nickel coating is modeled as a tube conductor, with an outer radius (r_{out}) of 4.5 μm and an inner radius (r_{in}) of 3.5 μm . The inductance is calculated as Equation 2 [30].

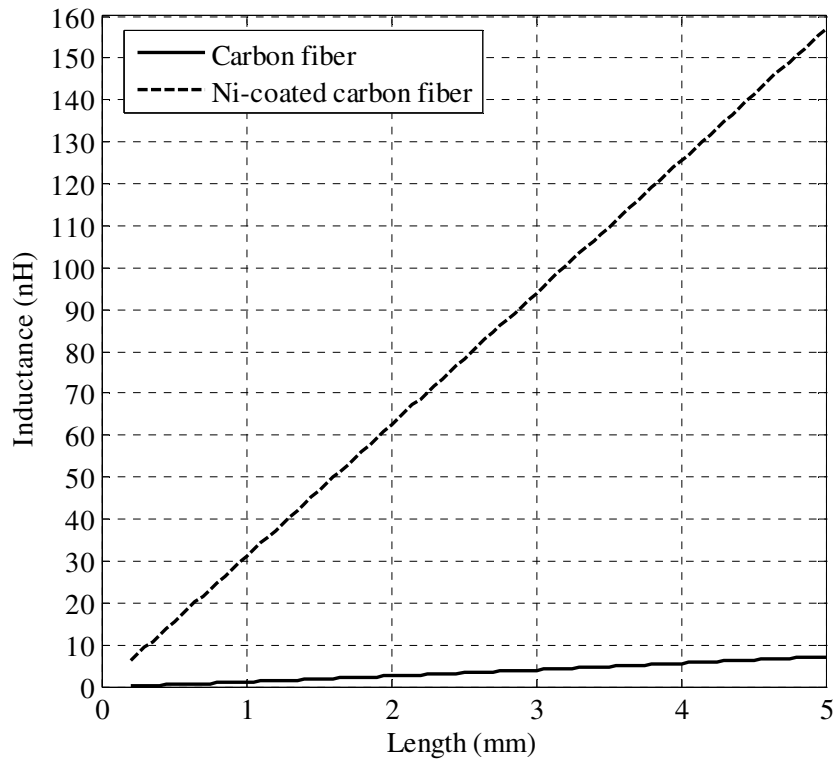
$$L_{tube} = 2 \cdot l \left(\ln \left(\frac{2 \cdot l}{r_{out}} \right) + \ln \zeta - 1 + \frac{\mu_r}{4} \right) \cdot 10^{-7} \text{ (Henry)} \quad \text{Equation 2}$$

where μ_r is the relative magnetic permeability ($\mu_r = 600$ for nickel), ζ is a geometry coefficient which is determined by the ratio of inner and outer radius. In this case, $\ln \zeta = 0.0663$ when $r_{in}/r_{out} \cong 0.8$.

The self-inductance vs. length results plain carbon fiber and nickel coated carbon fiber are plotted in Figure 12. The inductance is essentially proportional to the length. The inductance of bare carbon fiber and nickel coated carbon fiber are about 1.4 nH and 30 nH per mm, respectively.

The samples used in the experimental impedance analysis are 10-mm-long. Based on the analytical calculation, they are supposed to have the self-inductance of 14 nH (plain) and 300 nH (nickel-coated). Using the inductive reactance equation: $X=2\pi fL$, at the maximum frequency in the test, 2 MHz, their inductive reactance is 0.2 Ω and 3.8 Ω .

When a thousand carbon fibers are used in parallel, the total inductance would be one thousandth of the inductance of a single fiber, similar to the parallel resistance calculation².



² assuming no magnetic coupling.

Figure 12: Inductance of bare carbon fiber and nickel coated carbon fiber

4.1.5 Skin effect analysis

The skin effect is a phenomenon whereby the flow of alternating current, particularly at high frequencies, tends to concentrate near or at the surface of a solid conductor. Due to the reduced cross section area for current flow when skin effect occurs, the effective resistance of the conductor increases. A criterion to evaluate skin effect is skin depth, defined as the depth from the surface at which the current density is equivalent to 37% of the surface current density. Skin depth is determined by the resistivity (ρ) of the conductor and the frequency (f), as shown in Equation 3 [31].

$$\text{Skin depth: } d = \sqrt{\frac{\rho}{4 \times 10^{-7} \pi^2 f}} = 503.3 \sqrt{\frac{\rho}{f}} \text{ (m) where } \rho \text{ in } \Omega\text{-m} \quad \text{Equation 3}$$

For carbon fibers, skin effect becomes a concern when the skin depth is less than its radius. The skin depths of carbon fiber and nickel are plotted versus frequency in Figure 13. From the figure we conclude that, skin effect is not significant for carbon fiber when the frequency is below 300 GHz. For the nickel-coated carbon fiber, when frequency is over 20 GHz, the skin effects on the nickel coating may change the current distribution in the composite parallel conductor of nickel coating and carbon fiber. As a conservative consideration, carbon fiber with nickel coating is safe for the signals below GHz frequencies, including pulses signal.

In the experimental analysis, the maximum frequency is 2 MHz, which is lower than the critical frequency, the change in resistance is not expected, as the experimental result shows.

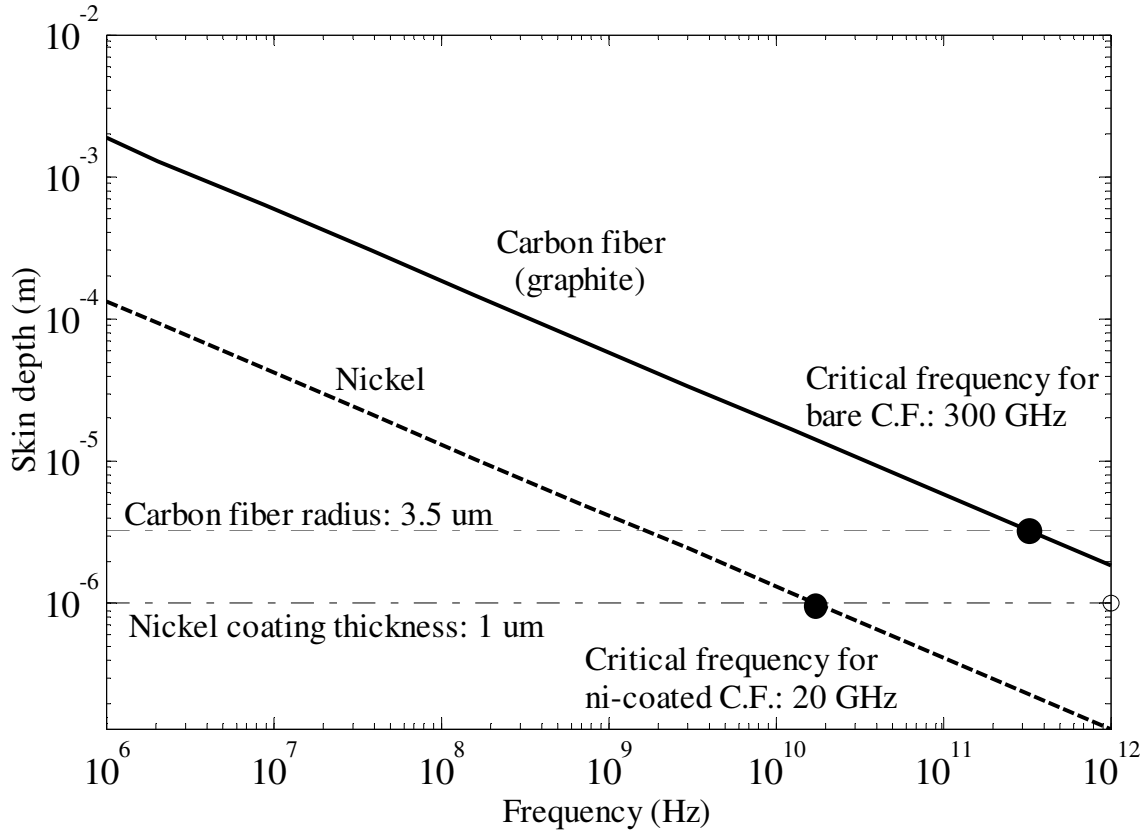


Figure 13: Skin depth versus frequency for different conductor materials

4.1.6 Conclusions

Due to the intrinsic resistivity of carbon fiber, resistance of carbon fiber is higher than commonly used metal conductors of comparable dimensions. Its resistance can be decreased by increasing the number of filaments, or applying a metal, such as nickel, coating over carbon fibers.

Carbon fiber bundle is more efficient in conductivity than carbon fiber composites, because manufacturing carbon fiber composite involves a pultrusion process (which is associated with cost) and consists of resin (> 9% in volume), which contributes weight but no conductivity and blocks redundant current paths between parallel carbon fibers.

Skin depth and inductance is not a limitation for carbon fiber, since a large amount of thin carbon fibers are always used parallel to form an interconnect. For metal conductors, this number of strands is not practical.

4.2 Solderability investigation

A permanent interconnect comprised of carbon fiber can be achieved by soldering if carbon fiber is solderable, or becomes solderable under certain conditions. Solderability tests (as per IPC/EIA/JEDEC J-STD-002B: Solderability Tests for Component Leads, Terminals, Lugs, Terminals and Wires [32]) were conducted.

Test samples included individual plain carbon fiber, individual nickel-coated carbon fiber, plain carbon fiber bundle (1,000 filaments), nickel coated carbon fiber bundle (12,000 filaments), carbon fiber composite rod consisting of plain carbon fibers (10,000 filaments), and carbon fiber composite rod consisting of nickel coated carbon fibers (10,000 filaments). The test was conducted on two types of solders: eutectic tin-lead (Sn63-Pb37) solder and a lead-free (Sn-3.5Ag-0.5Cu) solder.

The test sample was firstly dipped in flux for few seconds, which improves the wetting to solder, and dried in air for approximately 10 seconds. Then the tip (10 mm) of the test sample was dipped in molten solder, which was contained in a solder pot, for approximately 30 seconds, and then taken out. Visual and optical microscopy inspections were conducted to identify if there was solder adhered on the carbon fibers. Solder on test sample would indicate the possibility to make a solder joint. The result is listed in Table 4. Tests with both solders yield the same result: individual nickel-coated carbon fiber was solderable, as well as a bundle of nickel carbon fiber. A metal layer, such as nickel, is necessary to enable carbon fibers to be soldered. The carbon fiber composite rod made of nickel-coated carbon fibers does not wet to the solder because the nickel coating on fibers was surrounded by the epoxy resin (see Figure 5). The experiment results suggest that the

nickel coating enables the solderability of carbon fibers. CFC made of nickel-coated carbon fiber doesn't wet since the resin isolates the nickel surface from the solder.

Table 4: Results of solder wetting test

	Eutectic tin-lead (Sn63-Pb37) solder	SAC lead-free (Sn-3.5Ag-0.5Cu) solder
individual plain carbon fiber	No wetting	No wetting
individual nickel-coated carbon fiber	Wetting	Wetting
plain carbon fiber bundle	No wetting	No wetting
nickel-coated carbon fiber bundle	Wetting	Wetting
plain carbon fiber composite	No wetting	No wetting
nickel-coated carbon fiber composite	No wetting	No wetting

An experiment was setup to demonstrate the solderability of nickel-coated carbon fiber bundle. A bundle of 12,000 nickel-coated carbon fibers, secured in a plastic sleeve, has a 3-mm-long brush at the tip. Such a sample was managed to be soldered on a copper substrate at the brush. The copper substrate has a concave which helps to hold the solder. A fixture was made and used to fix the sleeved fiber bundle and copper substrate in position during the solder process (see Figure 14). A solder iron was used to apply the heat to melt the solder. Figure 15 shows a soldered sample. And Figure 16 shows the cross-section of the solder joint on the same sample. The solder penetrated into the fiber bundles during the soldering process.

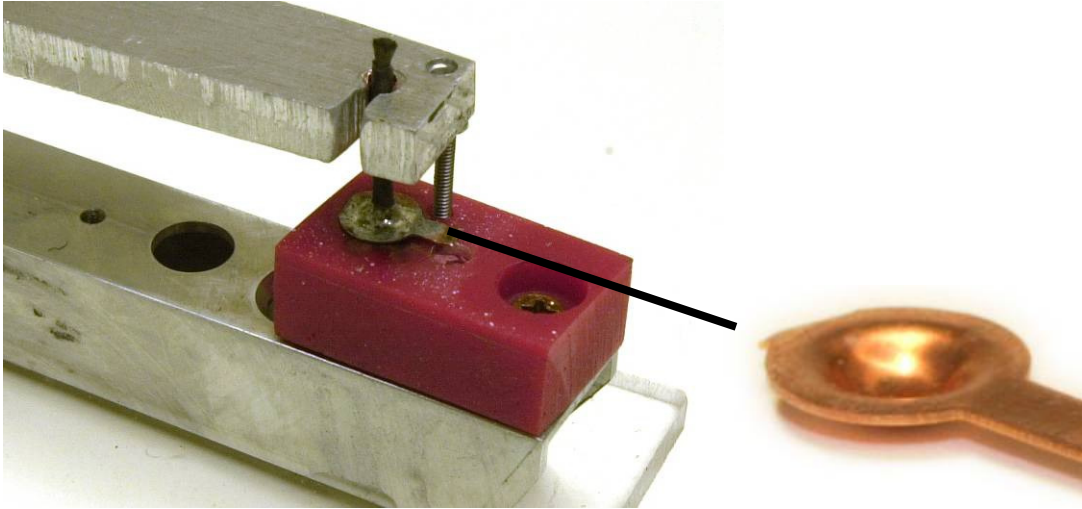


Figure 14: A fixture holding carbon fiber sample and copper substrate



Figure 15: A carbon fiber solder joint



Figure 16: Cross section of a carbon fiber solder joint

4.2.1 Solder joint strength evaluation

A tensile test was conducted to evaluate the mechanical strength of the previously made solder joint. 10 sleeved carbon fiber bundles were soldered to the copper substrates on both ends. For each test sample, there were two solder joints and two copper substrates. The two copper substrates were attached to the opposite test probes on a tensile tester (see Figure 17). An incremental displacement (elongation on test sample) was applied and the force was recorded. For every sample, one solder joint on either side was broken.

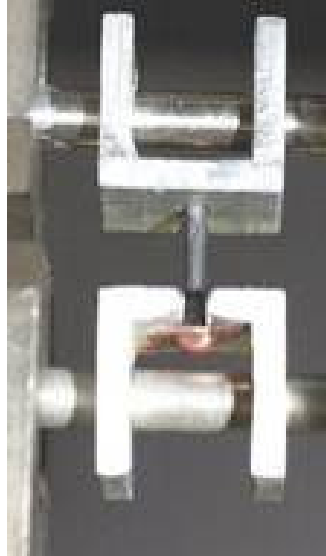
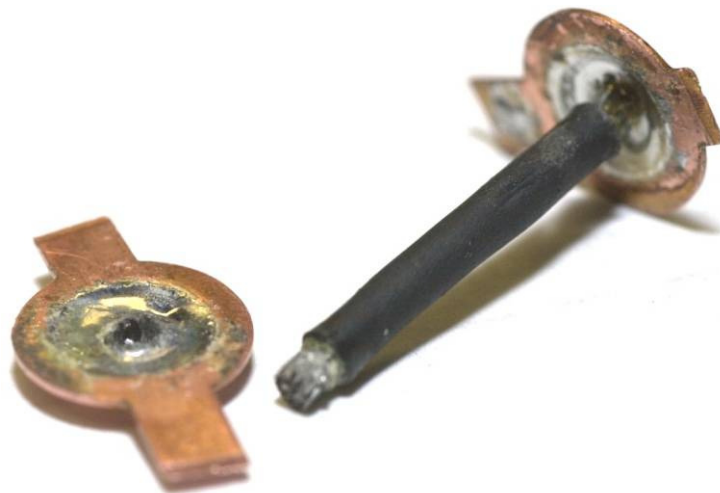


Figure 17: Test fixture for the tension test

Figure 18(a) shows a typical broken sample. Carbon fiber bundles were pulled off from the solder joints. the carbon fiber bundles did not break in the half. Microscopy image, Figure 18(b), indicates solder residue on the surface of carbon fibers. For the ten samples, the average force to break the solder joint was found to be 220 N, with a standard deviation of 133 N.



(a) Overview



(b) Close-up view of the carbon fiber bundle

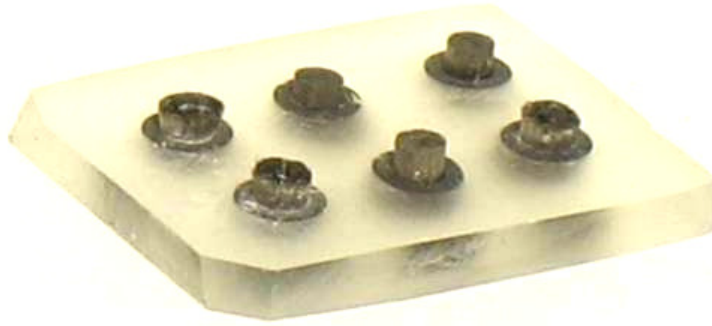
Figure 18: Broken solder joint after the tension test

The cylindrical surface between the carbon fiber bundle and solder joint is assumed to be the primary loading interface, because 1) the side surface between the solder bulk and fiber bundle was four times large as the circular area of the bundle tip, and 2) the nickel coating, which determines the wetting to the solder, was applied on the side of the fiber only, not on the tip. The loading surface is parallel to the loading direction, therefore a shear force is considered. The cylindrical area was measured to be $7 \times 10^{-6} \text{ m}^2$. Using the average breaking force 220N, the ultimate share stress in test was calculated to be 31.4 MPa by dividing the force by area. The ultimate share stress value is on same magnitude of the shear strength of Pb63-Sn37 solder (48 MPa [33]). That suggests that the bulk solder is the “weakest link”, and also that explains for the solder residue on the carbon fiber bundles. It is believed that the solder joint mechanical strength is sufficient for typical electronics applications.

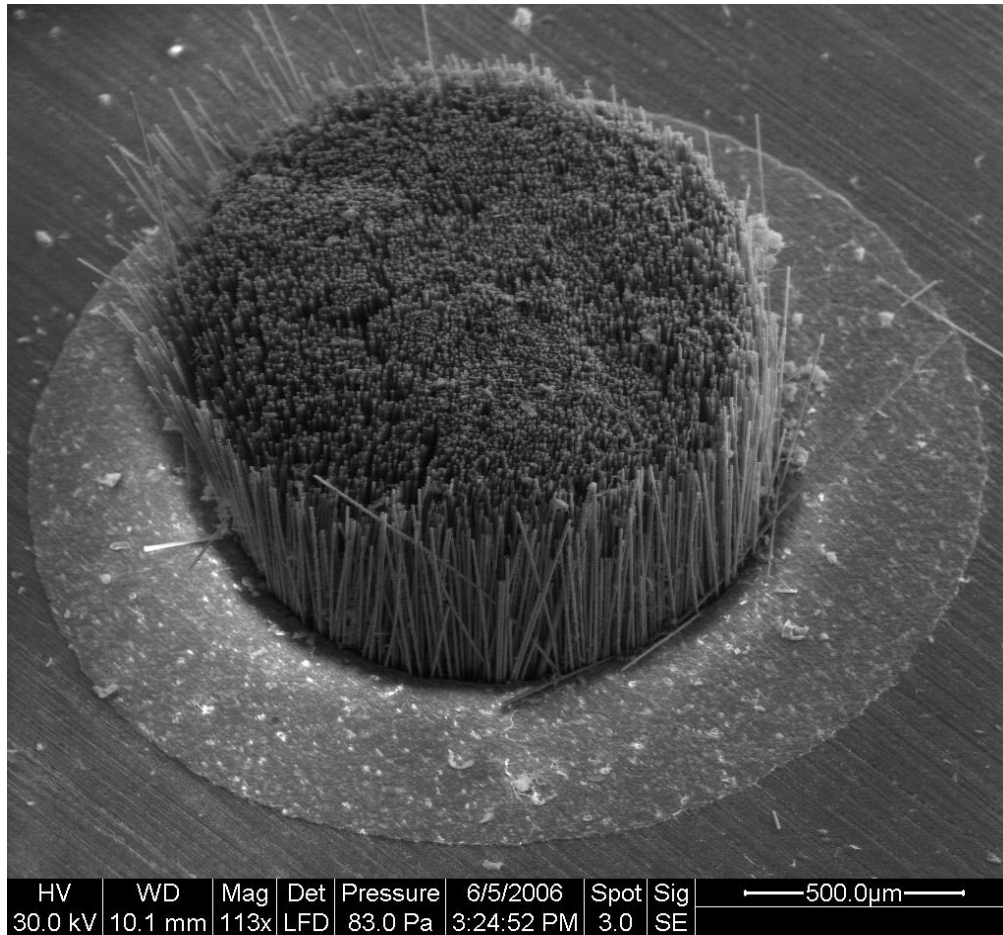
Chapter 5 PROTOTYPES

5.1 Overview

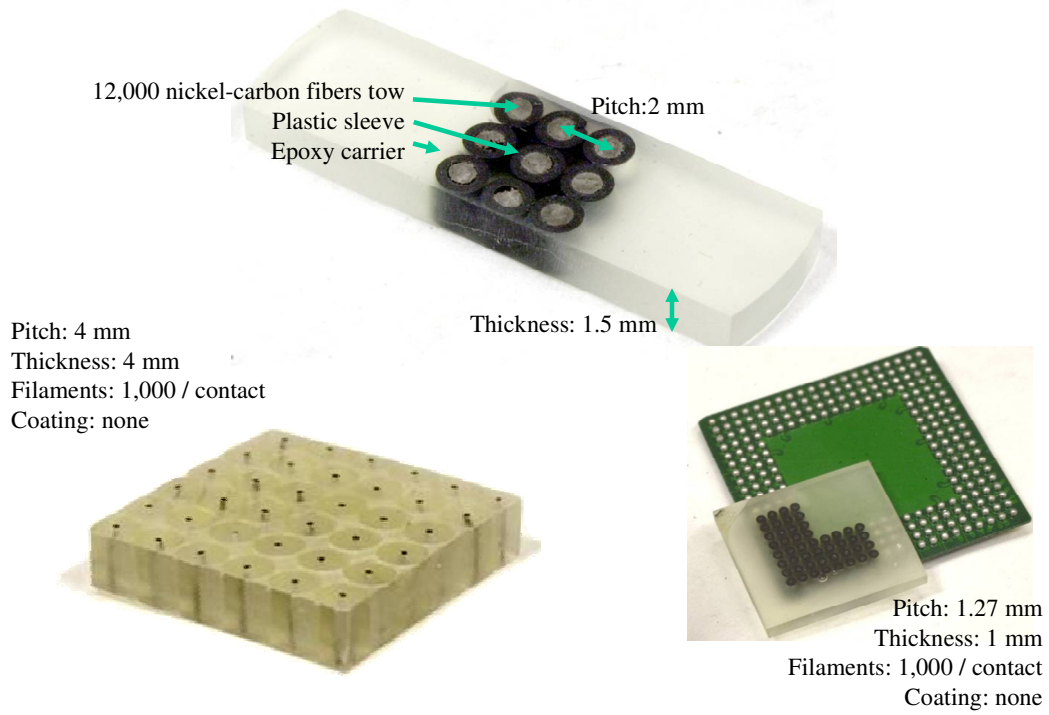
Several prototypes were fabricated in this research. These prototypes demonstrate the design concept, and more importantly, they make it possible to evaluate the performance of the interconnect device. Figure 19(a) shows a board-to-board interposer prototype consisting of a 4 mm-pitch 2x3 array of contacts, mounted in an epoxy carrier. Each contact was made of a bundle of 12,000 nickel-carbon fibers held in a plastic sleeve, as shown in Figure 19(b). Figure 19(c) shows some other prototypes. The essential elements of the interconnect device include the contact medium, the insulation sleeve, and the carrier.



(a) A board-to-board interconnect prototypes



(b) A contact pin, consists of 12,000 nickel-coated carbon fibers



(c) IC package to board interconnect prototypes

Figure 19: Prototypes of grid-array carbon fiber electronic interconnect devices

5.2 Contact design

The contact medium is carbon fiber bundle, sometimes coated with nickel. The prototype shown in Figure 19 (a) was designed to provide a bulk resistance of 1 m Ω . To achieve that target, each contact was designed to consist of 3-mm-long 12,000 nickel-coated carbon fibers. The length of the contact is designed to be greater than the thickness of the socket carrier, in order to achieve a brush-like soft tip. The purpose of this design is to minimize the contact resistance and provide a contact wipe.

5.2.1 Contact resistance

A soft, brush-like surface is designed into the carbon fiber contacts, as opposed to a harder, rigid surface which is also possible. A soft contact interface allows a larger fraction of fibers to contact the pad and results in lower contact resistances [26][27]. A carbon fiber brush has been shown to form naturally at the tip region if the fiber bundle protrudes from the sleeve a sufficient distance.

Carbon fiber composites (CFC) is not selected in this research due to some concerns. CFCs are typically described as rigid, conductive plastics. As such, CFCs tends to exhibit electrical contact resistance properties similar to metals. By using a suitable CFC and resin-removal process, it is possible to convert the relatively hard CFC into a very soft, and compliant carbon fiber brush that can be suitable for use as an interconnect material. For carbon fiber composite rods, removing the binder resin from a small area at the contact location can establish a surface contact region that contains nearly all fiber and result in a soft brush-like tip. The resin can be removed by exposing the CFC to intense local heat, such as a flame or a laser or by chemical removal. Laser heating or flame heating has been shown to remove the resin, but care must be taken to avoid

removing any metal coating that may be on the fibers. When properly done, the carbon fibers become free from the binder polymer that comprises the CFC and can act as a multiplicity of independent contact elements. Figure 20 shows a typical brush-like structure made from a 1.6 mm diameter CFC rod where the surface was prepared by exposure to a flame. Subsequent to resin removal, a sleeve can be used to reconfigure and hold the bundle of fibers together in the desired shape.



Figure 20: A carbon fiber composite rod with a brush at the end

5.2.2 Design for contact wipe

Certain degree of contact wipe is preferred for a separable interconnect interface, because it can help to remove or displace contaminants on the contact pads, such as dust or other particulate debris, and thus ensure a cleaner, low contact resistance interface. During insertion of a fiber-based interconnect, the brush fibers are able to bend in

response to a slight compressive force. Thus the multiplicity of fiber tips can wipe over the contact pads on both the packaged device and printed circuit board.

An experiment was conducted to demonstrate the wipe motion. A prototype with one carbon fiber contact was used. The tip of the carbon fiber bundle was compressed under glass, through which the contact surface was visually observed and video taped. Key images during the process are shown in Figure 21 and Figure 22.

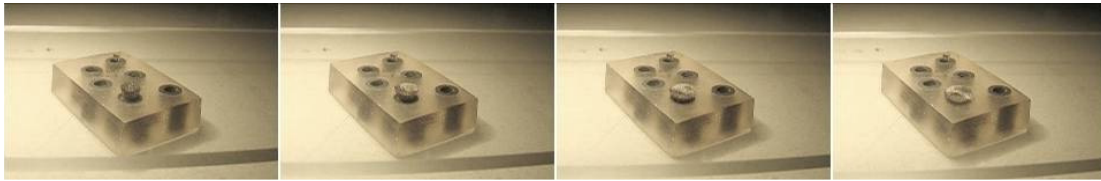


Figure 21: A carbon fiber brush being compressed by a piece of glass

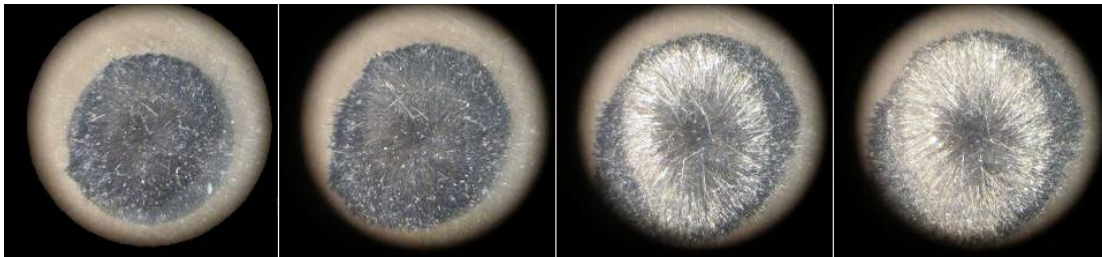


Figure 22: Close-up of a carbon fiber brush being compressed by a piece of glass

The contact region starts as a solid circle in the early stage of contact. The fibers contact the pad with the tips, which are perpendicular to the pad. As the fibers are compressed, the contact region forms a ring, with the fibers bent towards the outside. The inner fibers become parallel to the pad, and they contact the pad with their sidewalls. Namely, the nickel coating on individual fibers is in a preferred contact with the pad. Meanwhile, the fibers on the outside bend away from the pad, since they are pushed by the fibers from the inside. During the whole process as the carbon fiber contact is compressed against a flat pad surface, the fiber brush dispersing out, individual carbon fibers bend towards the outside, and their tips slip (wipe) on the pad surface. The exact

wipe motion depends on the fiber brush length, the number of fibers in bundle, the bundle diameter, the mechanical characteristics of the fiber and coating, and the smoothness of the pad. Further study can be carried out to quantify the effects of these factors.

5.3 Insulating sleeve and carrier

The insulating sleeve is to protect and restrain the carbon fiber bundle and prevent them from losing. In the prototypes fabricated, silicones and heat shrinkable tube was used. An insulation coating on the bundle may be considered as well.

The carrier has several purposes: electrically insulates contact members, mechanically supports contact members and maintains them in position, exerts and maintains contact pressures, shield contact members from the operating environments; provides mechanical protection for the contacts. In this prototype, epoxy was used to form the carrier. The carrier can be made of various of materials, such as silicone, nylon, polyamide (PA), ABS, polyimide (PI), polycarbonate(PC), polyvinylchloride (PVC), polyvinylacetate (PVA), polyethyleneterephthalate (PET), polybutylterephthalate (PBT), polyetheretherketone (PEEK), polyphenylsulphide (PPS), polyurethane(PU), polyethylene (PE), polypropylene (PP), polystyrene (PS), polytetrafluoroethylene (PTFE), phenolic, epoxy, and copolymers, blends, mixtures and composites. The carrier should be attached to the printed circuit board using certain approach, such as bolts and alignment keys. Accessories, such as heat sink, heat spreader and cooling fan may be attached to the socket carrier.

5.4 Fabrication process

This section explains the detail procedures of fabricating a carbon fiber interconnect prototype, using the prototype shown in Figure 19(a) as an example.

5.4.1 Contact preparation

Carbon fiber is the raw material for the contact. It is commercially available as bare carbon fiber bundle and nickel-coated carbon fiber bundle, which are usually wound in reels. The fiber bundle was put inside a heat shrinkable tube, which was originally thick enough to contain the fiber bundles. The heat shrinkable tube with fibers inside was chopped to approximately 50-cm-long each piece. Then these chopped segments were subject to an elevated temperature to shrink the tube and therefore make the tube holding the fibers tightly. The shrunk tubes with fibers were then chopped again to pieces of 3 to 4 cm, as raw contacts for the next steps.

5.4.2 Molding

The raw contacts were then to be molded in an epoxy carrier. A plastic mold was used for the molding. The mold consists of a cylindrical tube and two end caps, as shown in Figure 23. Both of the caps have arrays of holes, which are to fix the raw contacts in an array, as Figure 24 and Figure 25 shows. The uncured epoxy with hardener was then filled into the mold.



Figure 23: Mold for the fabrication of carbon fiber socket prototype



Figure 24: Raw contacts in the mold

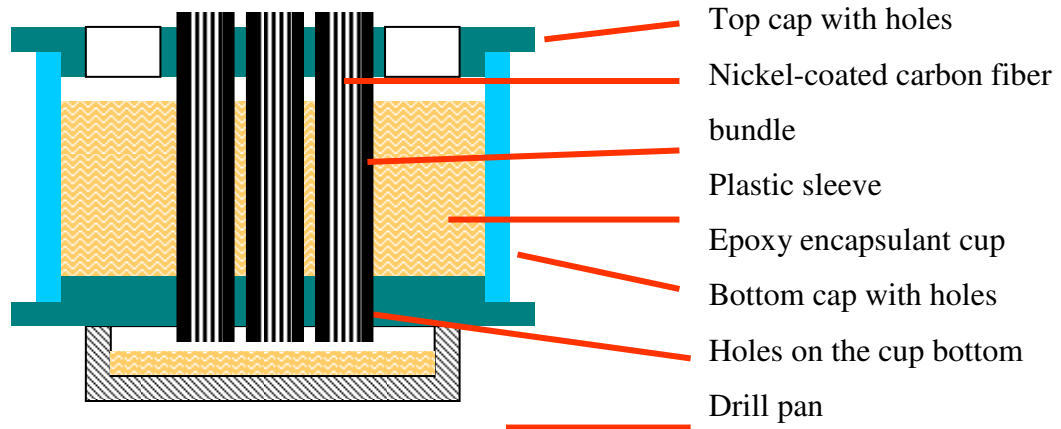


Figure 25: Cross-section illustration of the mold in encapsulation

5.4.3 Trimming and slicing

Once the epoxy cured, the epoxy became a rigid bulk with raw contacts distributed in it, which is referred as molded raw contact. The molded raw contact was removed from the mold, and then trimmed by cutting off the protruding fiber bundles and other protruding portions. The trimmed molded raw contacts were then sliced cut to pieces of several millimeters using diamond saw. Several pieces can be made from one molded raw contact. Each piece was to form one interconnect device prototype.

5.4.4 Contact surface preparation

The slices of molded raw contact were then grinded on sand papers to remove the sleeve and epoxy carrier around the fiber bundles for a small depth (e.g. 0.5 mm on each side) to make the fiber bundles protrude and therefore form brushes.

5.4.5 Ultrasonic cleaning

Finally, an ultrasonic cleaning was performed on the prototype to remove the debris during the previous steps, especially when diamond saw cutting and grinding was involved.

5.5 Automated manufacturing process – water-jet cutting

In the prototype fabrication, diamond saw cutting was currently used to slice the molded raw contact. However, it is a slow process since polishing and cleaning is necessary after this process, which might not be appropriate for actual production. Water-jet cutting may be an alternative fabrication approach, especially for automated mass production in industry. A water-jet cut was attempted with OMAX Model 2652 CNC abrasive water-jet cutter. Figure 26 shows the surface after a water-jet cutting.

Laser cutting had been considered as well. However, the high local temperature due to laser cutting could damage the metal coating, and may change properties of the carrier and sleeve. Water-jet cutting doesn't induce heat.

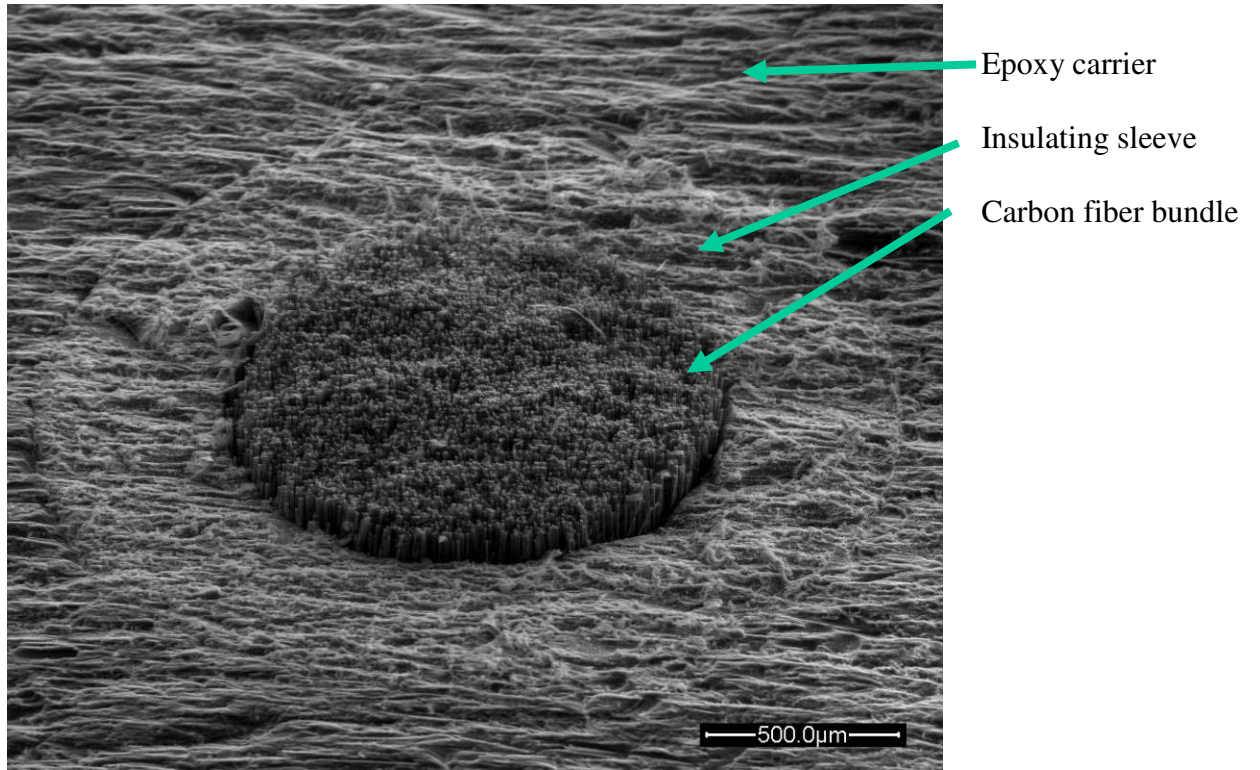


Figure 26: Surface processed by water-jet cutting

Chapter 6 PROTOTYPE CHARACTERIZATION

6.1 Mechanical characterization

When a separable electrical contact is in operation, a normal compressive force at the contact surface is required to ensure the contact and therefore provide the electrical path. For the carbon fiber interconnect, the normal force is applied to keep the carbon fiber contacts in touch with the metal pads.

Since the carbon fiber brush deflects subject to compression, it is important to discover the physics at the contact surface. Experimental investigation was performed in this chapter, including deflection - force relationship and the effect of multiple deflection cycles.

6.1.1 Force-deflection relationship

The force - deflection relationship of individual carbon fiber contacts was characterized using a compression test on a dynamic mechanical analyzer (DMA). 5 samples with different brush height were tested, which were labeled as A (shortest brush height, 0.45mm) through E (longest brush height, 1.15 mm).

The test sample was placed between a pair of planar probe, as Figure 27 shows. The lower probe is fixed and the upper probe can move in z (vertical) direction. The carbon fiber bundle protruded from the carrier only on the upper side, namely, there's only one brush for each prototype in this test. The gap distance between the upper probe and the carrier is defined as probe height, which also is the deflected brush height. The probe height was controlled in the test. The upper probe was reset to right above the brush before each test, and moves down to deflect the brush. The force on the probe was

recorded in real-time during the test. The test was ended when the load reached 300 grams. The probe-height vs. force result for all samples are displayed in Figure 28, and the detailed plots for Sample A and B are shown in Figure 29.

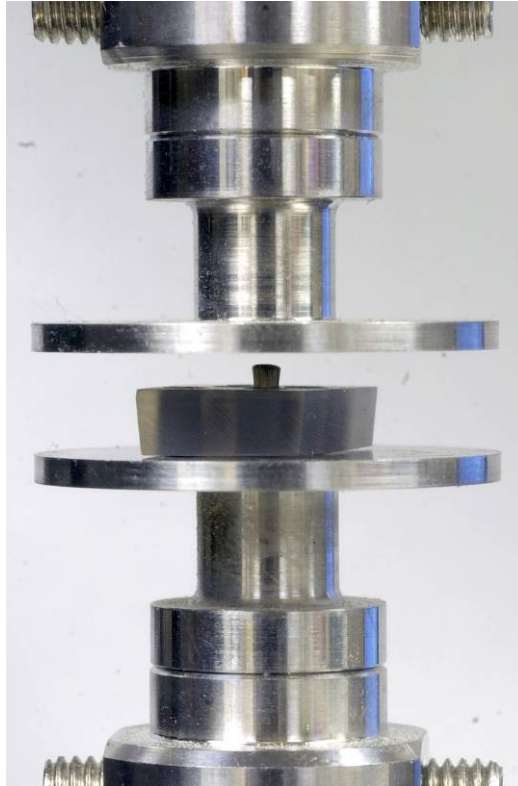


Figure 27: Test probe and contact under test

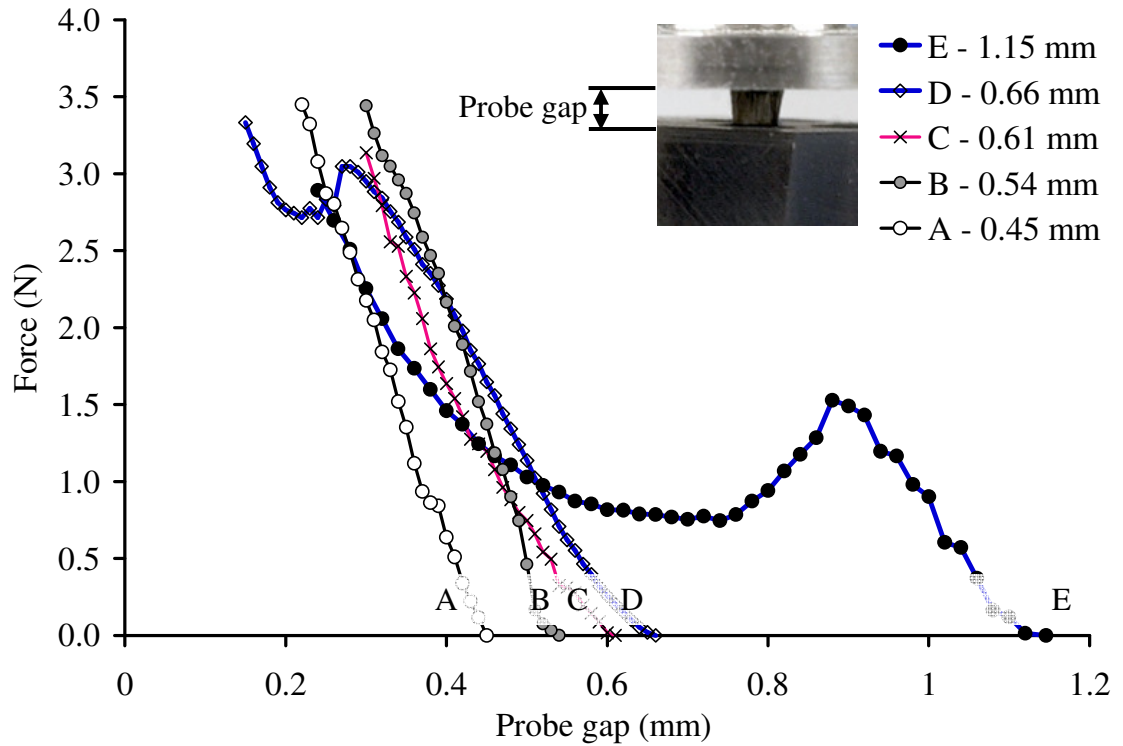


Figure 28: Force-Deflection Result - All Samples

The force-deflection behavior of Samples A and B appear essentially linear. The results for these two samples were replotted in Figure 29 for a detailed expression. Linear correlation was applied to calculate an effective stiffness for the sample contacts. The coefficients of correlation, which are greater than 99%, confirm the linearity of the force-deflection behavior of the carbon fiber brush contact.

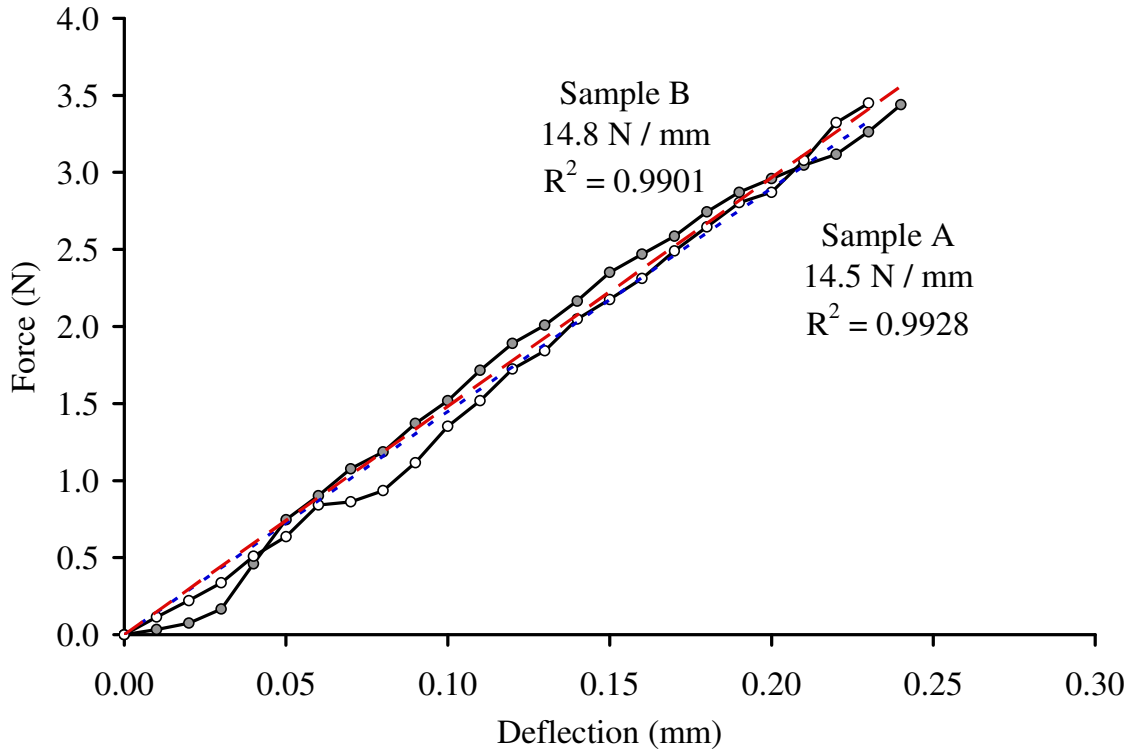


Figure 29: Force-Deflection Result - Samples A and B

Figure 30 shows a complete loading and unloading cycle of a test sample (A). The data points appear as a loop. Such a counter clockwise loop in a force-displacement plot indicates an energy loss from the system. The energy loss may be due to the plastic the friction between the fibers and the friction between the fiber tips and the contact pad.

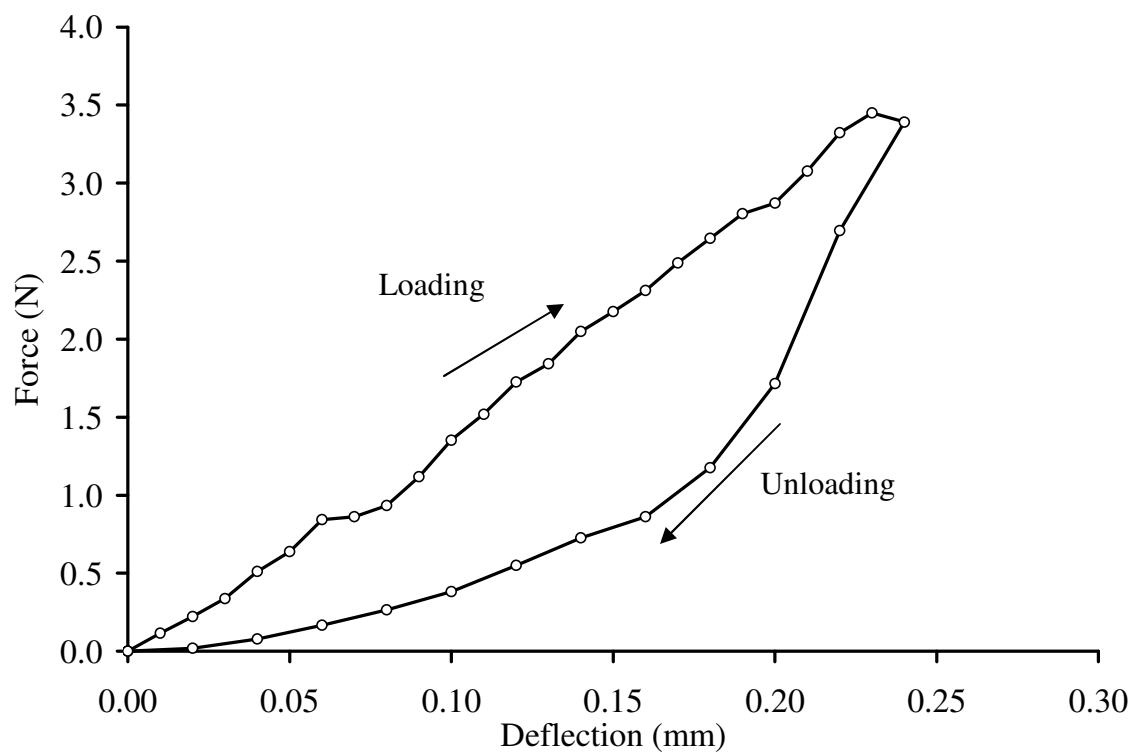


Figure 30: A cycle consisting of loading and unloading indicates an energy loss

For samples with longer brushes, Samples D and E, their force-deflection behavior was not monotonic as the rest of samples. Figure 31 shows the test plots accompanied with the images of the sample at associated deflection. The force-deflection is not on a one-to-one mapping, namely, applying a certain compression force does not always lead to a certain deflection condition. In the applications where a contact load is controlled, this uncertainty may impact the contact performance. Therefore, in the design of an interconnect device, this behavior should be avoided.

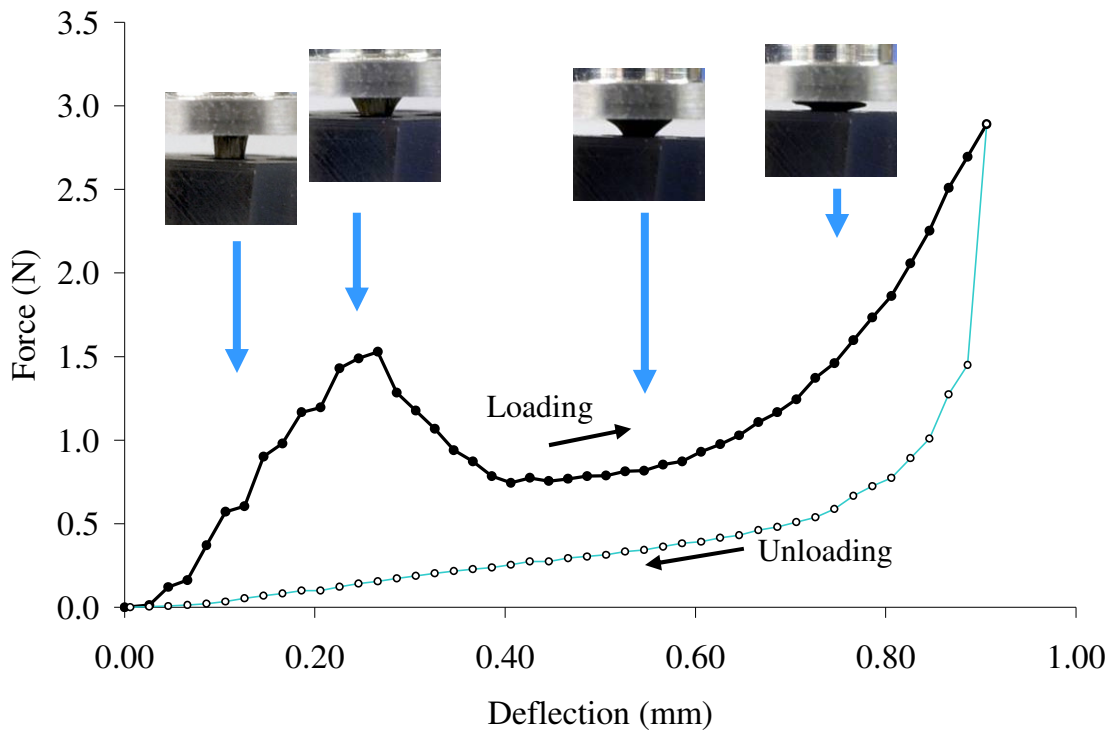


Figure 31: Force-deflection result - Sample E

6.1.2 Cyclic loading test

For a separable contact, it is important that it can survive a certain number of mating cycles (insertion cycles) during assembly and disassembly processes, especially if used as burn-in and test sockets. To assess cyclic loading, a test was performed, whereby

a prototype consisted of 6 carbon fiber bundle contacts, each with a 0.5-mm-long brush on each side.

A prototype with 6 contact pins were tested (see Figure 32), and subject to a cyclic load from 0 to 3.6 N (0.6 N per contact pin), for 100 cycles. The loading profile is shown in Figure 33. The force-deflection data of first 5 cycles is plotted in Figure 34.

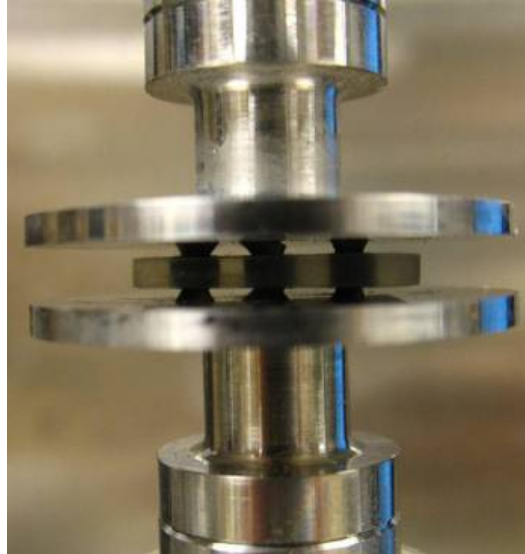


Figure 32: Probes and prototype under test

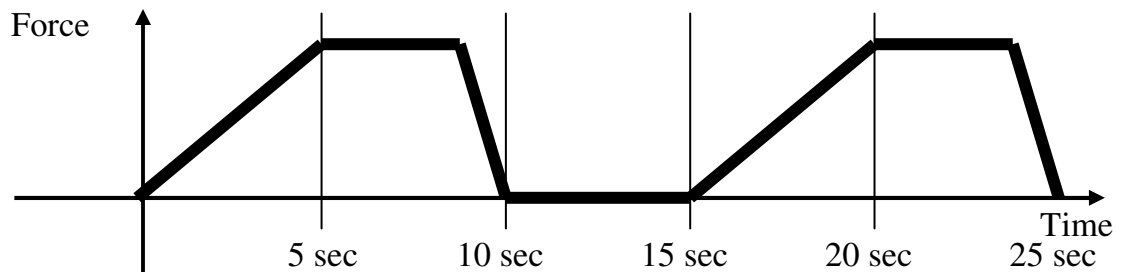


Figure 33: Loading profile

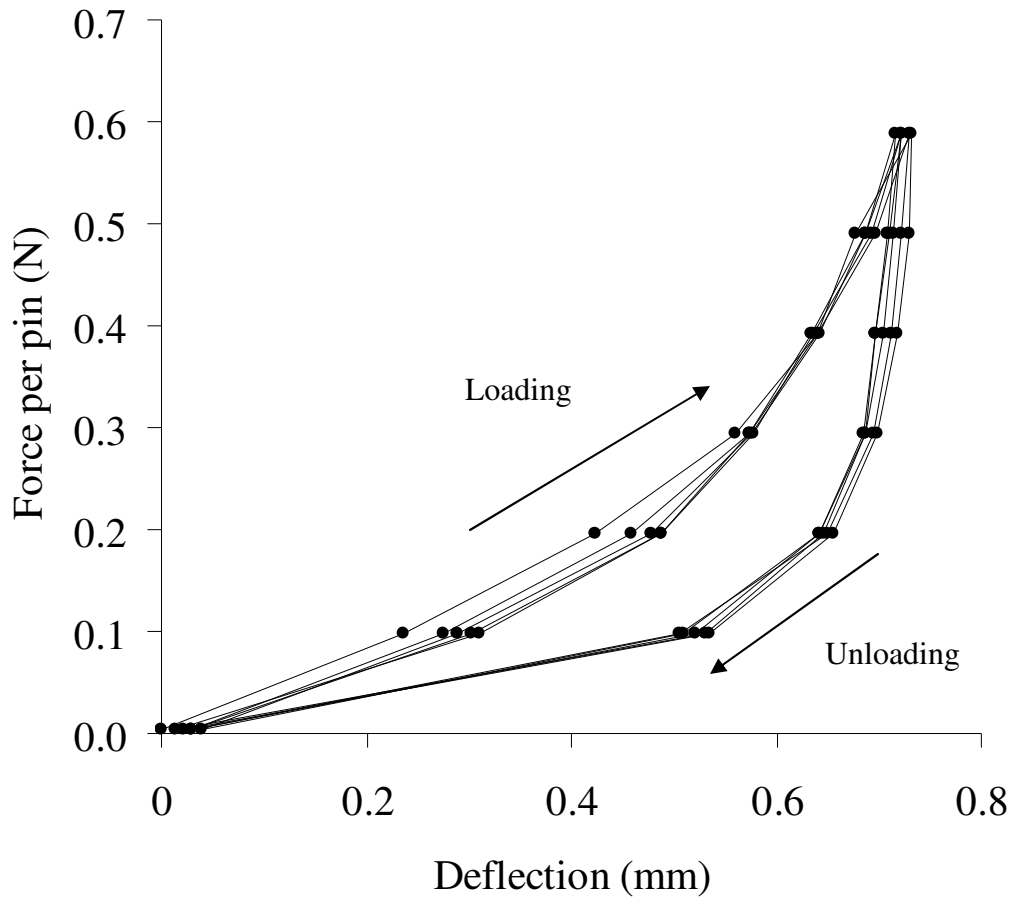


Figure 34: Force-deflection result of first 5 cycles

The carbon fiber contacts were observed with scanning electron microscope before and after the test. Figure 35 and Figure 36 show the same contact before and after the test, which are typical to represent the all 6 contacts in the prototype. No significant difference was observed, which indicates that no visible damage occurred from the test of 100 loading cycles. The contact probe showed no wear and debris.

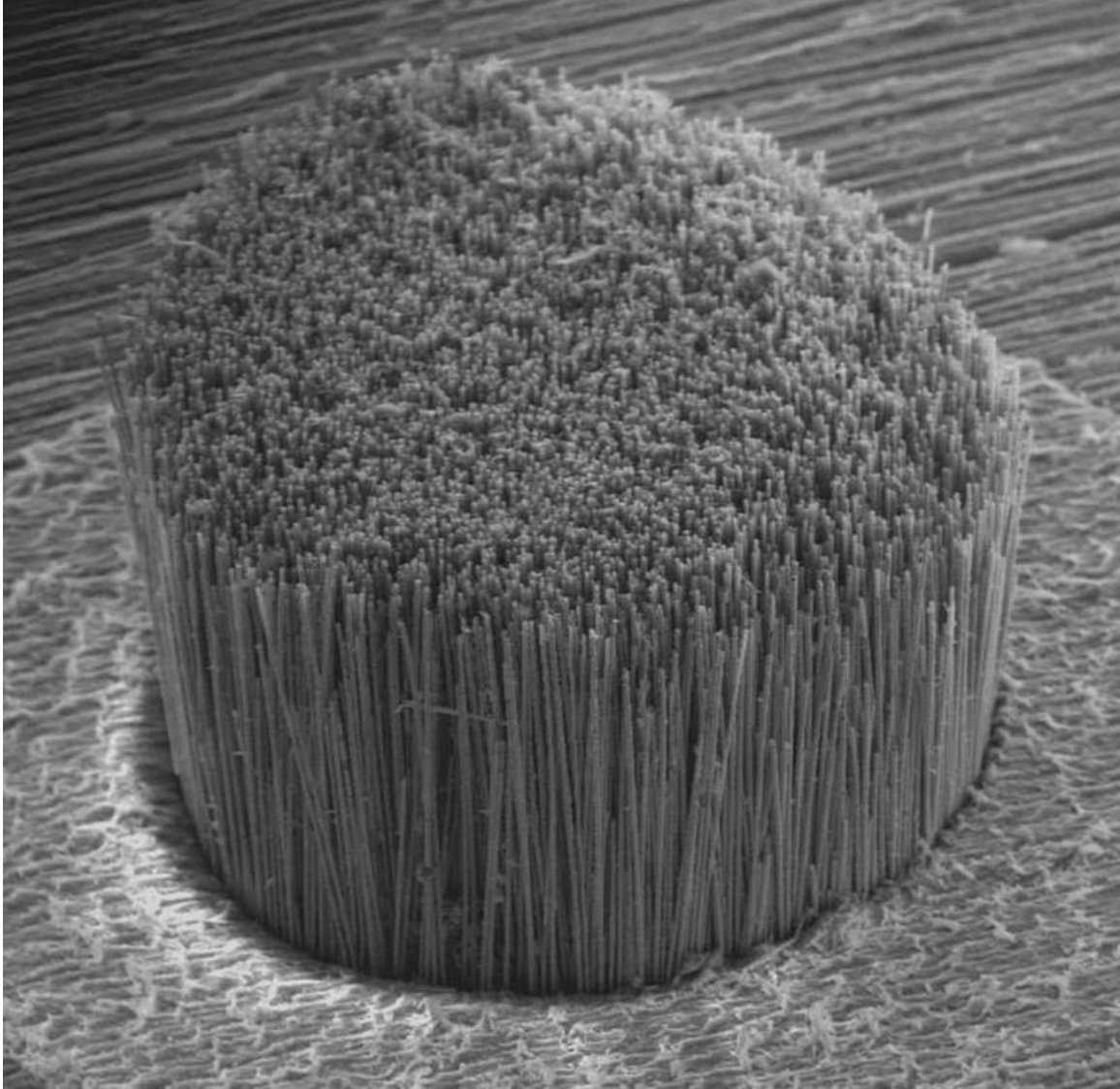


Figure 35: Microstructure of a contact before the cyclic loading test

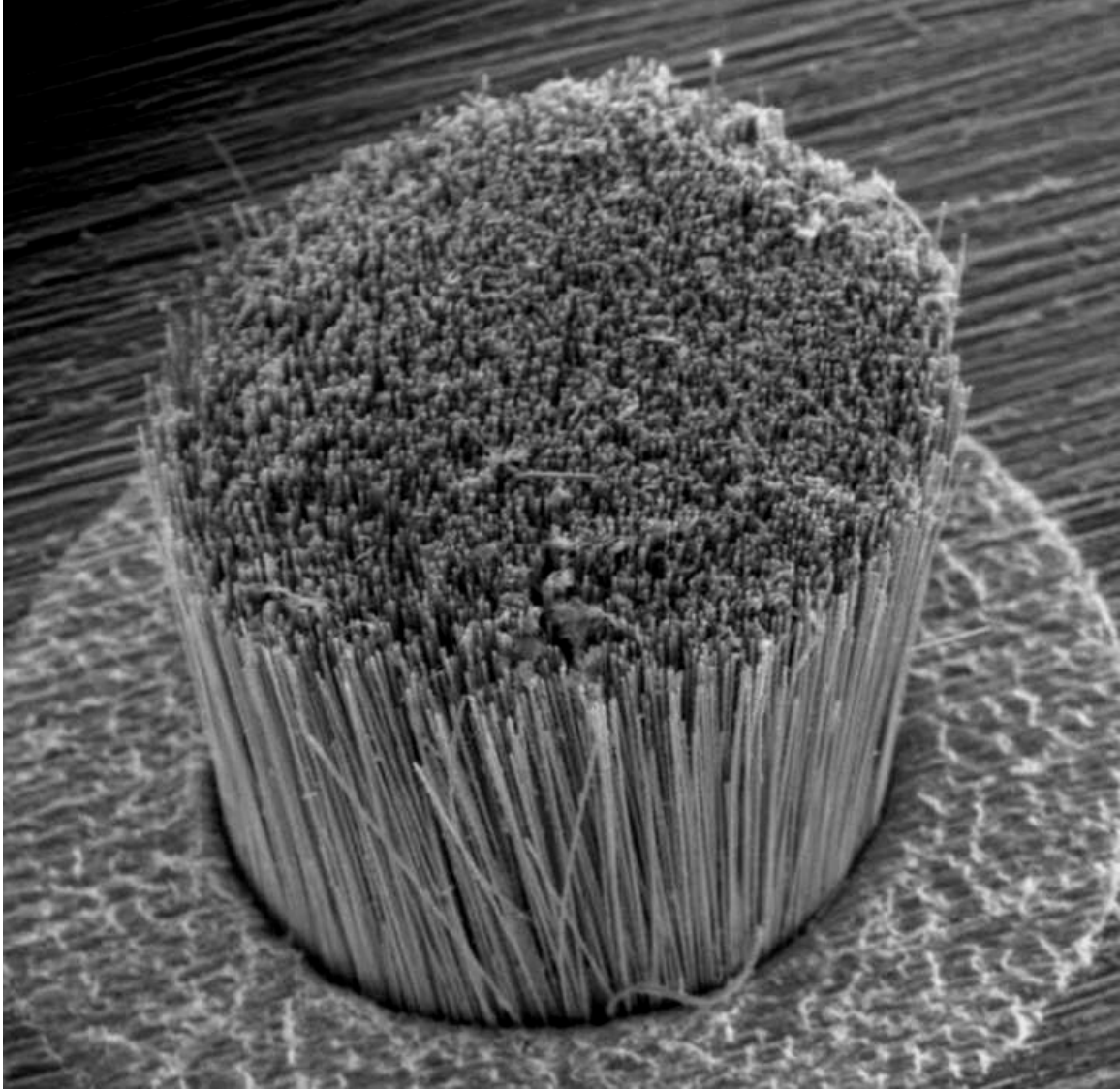


Figure 36: Microstructure of a contact after the cyclic loading test

6.1.3 Shear deformation due to CTE mismatch

In applications of IC package-to-board interconnection, when temperature changes, normally increases in operation, the packaged IC and the board expands on different scale, due to the CTE mismatch of the package and the board. For BGA interconnection, which has solid connection throughout the solder joint, the difference in thermal expansion induces an out-of-plane warpage and the solder joints are stressed. In the proposed design, which has at least one separable contact interface, a small amount of

in-plane relative motion is tolerated, as long as the carbon fiber contact pin stay in touch with the land pads on the IC package and the board.

Figure 37 gives an example of an interconnect device with an $N \times N$ array contacts. The contact center to center pitch is defined as p . The contacts at the corners are considered as critical contacts, since they are located at where the maximum expansion difference occurs. In some cases, the contacts near the ‘die shadow’ are considered as critical contacts as well. Such a case is not discussed in this research for simplification.

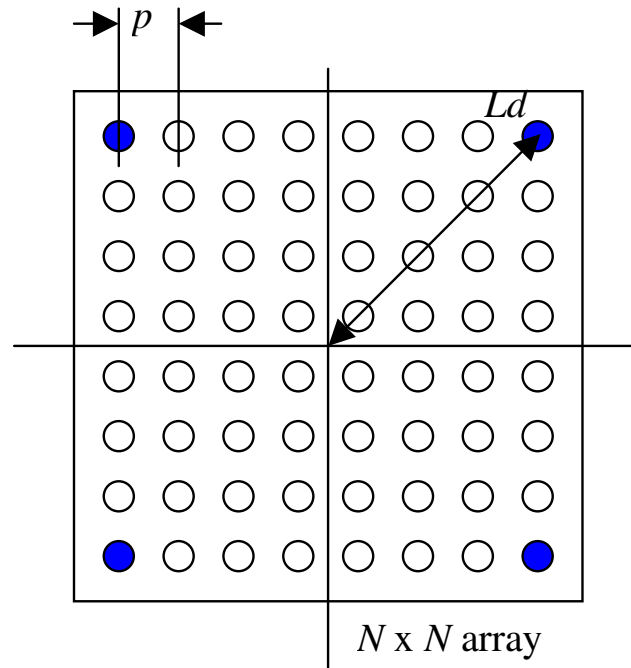


Figure 37: A schematic top view of a $N \times N$ array interconnect

The distance from the corner contacts to the package center is defined as Ld , which can be calculated from

$$Ld = \sqrt{2} \cdot \frac{N-1}{2} \cdot p \tag{Equation 4}$$

Figure 38 shows a schematic cross-section view along the center and one corner contact. The relative movement between the IC package pad and board pad at the corner, defined as pad offset Δx , can be calculated using,

$$\Delta x = Ld \cdot \Delta T \cdot \Delta \alpha \quad \text{Equation 5}$$

where ΔT is the temperature change and $\Delta \alpha$ is the CTE difference between the IC package and the board.

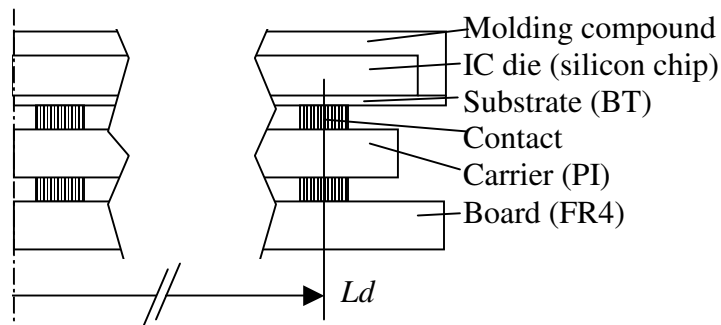


Figure 38: A schematic cross-section view along the center and one corner contact

For example, the array layout is 16 x 16 with 2.0 mm pitch. The diameters of the bundle contact and the land pads are 1.3 mm and 1.5 mm respectively. Based on Equation 4, Ld is calculated to be approximately 21 mm.

The FR-4 board has a CTE of 15 ppm/°C. A housing material can be chosen to match the board's CTE, such as polyamide. The package's thermal expansion is assumed to be dominated by the silicone die, which has a larger modulus than the molding compound and substrate and occupies the most volume of the package. Assuming the CTE of the silicone die is approximately 5 ppm/°C. The CTE difference is 10 ppm/°C. A 100°C temperature change is assumed. The pad offset for the corner contact can be calculated based on Equation 5. In this case, the calculated result will be approximately

0.02 mm. Considering the 0.2 mm diameter difference between the pads and contacts, such an offset will not bring a disconnection, as Figure 39 shows.

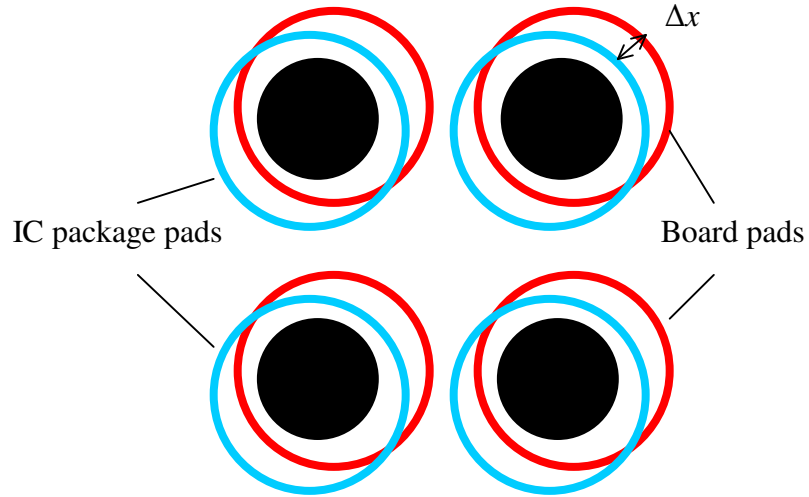


Figure 39: Pads offset due to CTE mismatch does not affect the contact integrity in this case

6.2 Electrical resistance characterization

Resistance of carbon fiber interconnect device prototype was characterized. Since the primary of the device is to conducting current, the resistance is the most important parameter to be evaluated. In the applications as separable interconnects where the carbon fiber contact conducts current between a pair of metal pads, the effective resistance is a sum of the bulk resistance of carbon fiber bundle and the contact resistance contributed by the interface, which is a dependant of the normal force applied on the interface.

The resistance characterization on the carbon fiber interconnect device prototype was performed with a test fixture (see Figure 40). The test fixture consists of a pair of boards and a switching circuit, (diagram shown on Figure 41). The boards were to connect the device under test, a interconnect device which has 6 contacts (2x3 array). Board B is fixed on the base. This is where the DUT sits during the test. It has six individual electrodes for six contacts. One contact will be measured at a time. A switch is used to select the contact for measurement. Board A is sitting on the DUT. It is guided by two screws to eliminate the in-plane movement. Different amount of weights are placed on the board to provide certain normal force at the contact interface. The top board has an electrode to contact all the six contacts of the interconnect device. The measurement was done by a digital multi-meter, with a 4-wire-connection (Kelvin) method: two wires go to the top electrode, two wires go to the bottom electrode through the switch.

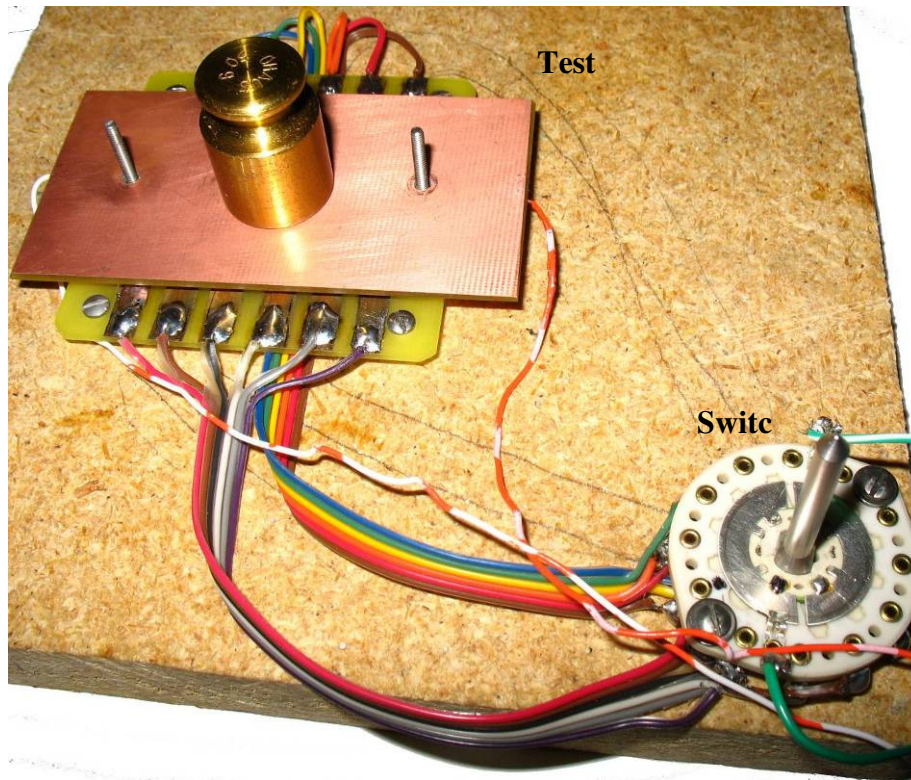


Figure 40: Test fixture for resistance characterization of the prototype

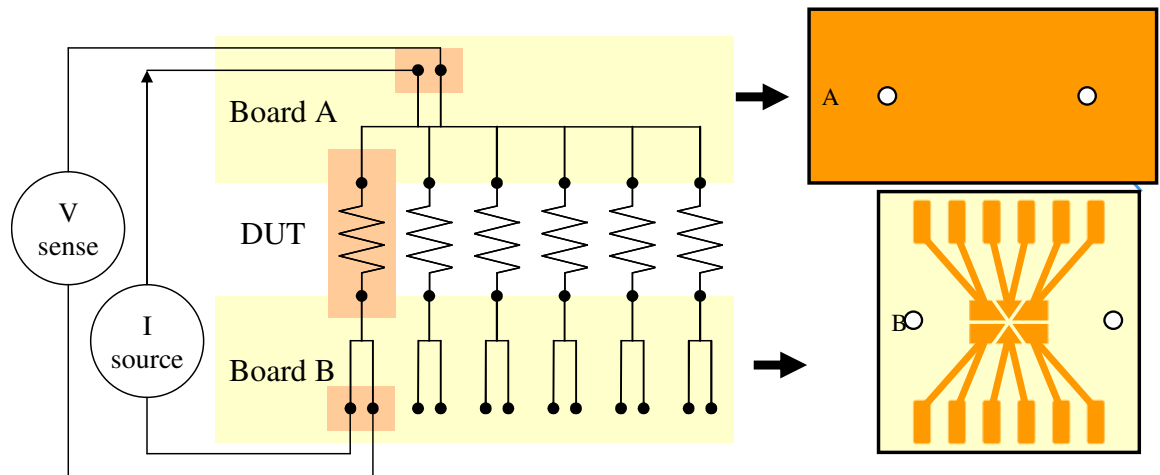


Figure 41: Diagram of the test circuit

An incremental force from zero to 0.67 N (70g) on each contact was applied in this test for two loading and unloading cycles. Typical resistance values are plotted in Figure 42 and Figure 43 (log-log).

The resistance across the prototype device was observed to fall below 400 mΩ when the force was greater than 0.1N. It is suggested that the force in application should be no less than 0.1N. Resistance values centered around 200 mΩ when the load was greater than 0.3N. The force-resistance behavior of the carbon fiber interconnect can be approximated as a power function, whereby Resistance (Ω) = 0.090 * Force (N)^{-0.86}.

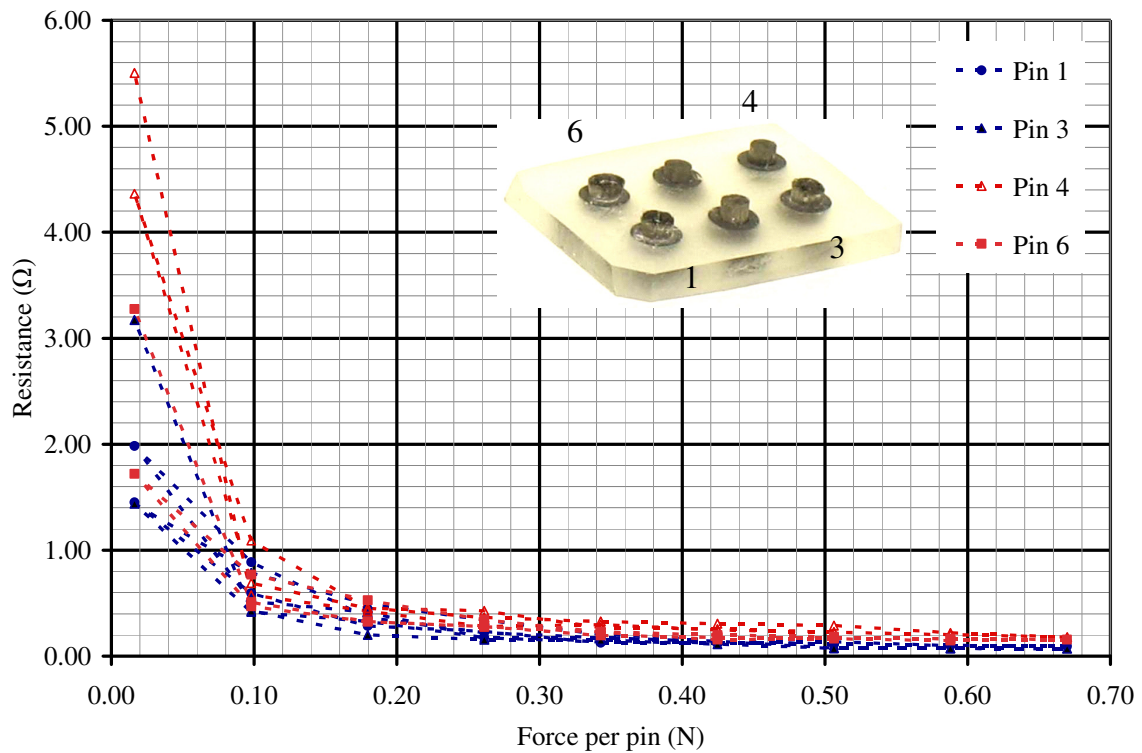


Figure 42: Resistance-load characterization result (raw)

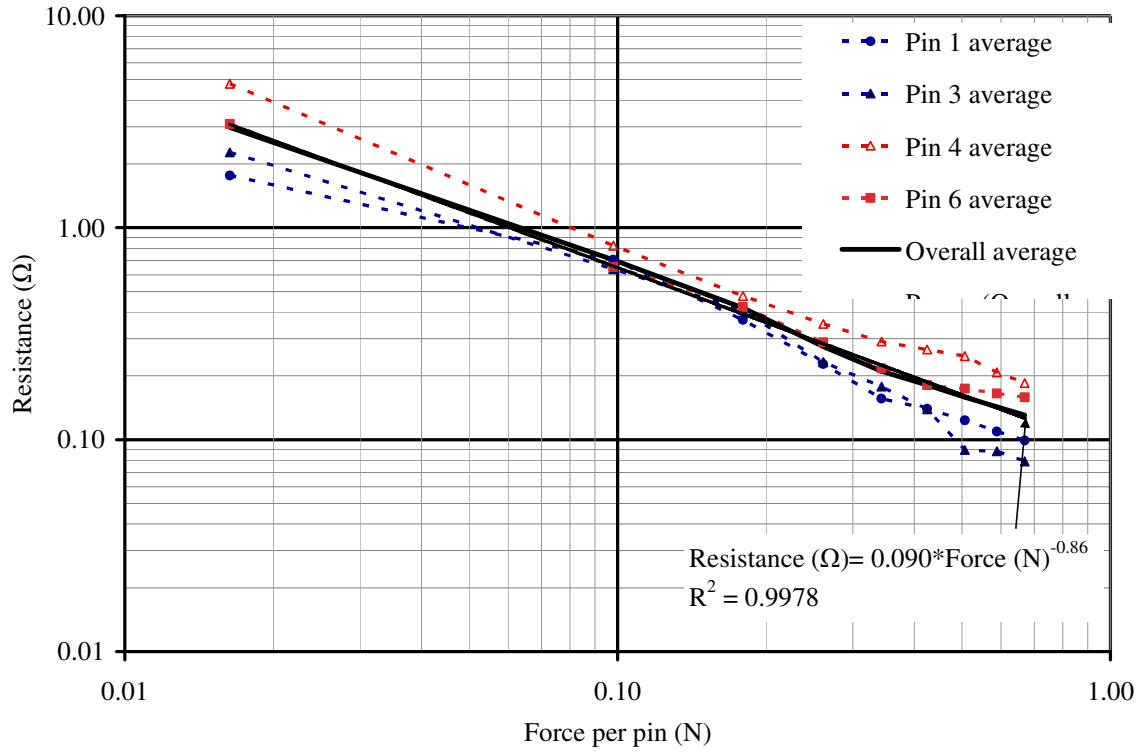


Figure 43: Resistance-load characterization result (averaged, log-log)

The force-resistance correlation might not necessarily be valid for extended force range. When the force is above certain level, the resistance will saturated to the bulk resistance, or, in some cases, the fibers might break and lead to a higher resistance.

Chapter 7 SUMMARIES

This study indicated that an inter-plane grid-array interconnect device, constructed by nickel-coated carbon fiber bundle could be developed and can be successful. Such an interconnect device can provide interconnection between two planar surfaces from a combination of semiconductor die, substrates, packaged components or printed circuit boards.

7.1 Advantages

The carbon fiber interconnect is believed to have the features of low contact wear, low contact force, contact redundancy and contact wipe, and therefore it provides a stable and reliable electrical connection. For high speed applications, the carbon fiber-based interconnect is believed to outperform single strand conductor-type interconnects due to its low inductance.

Also, carbon fiber is thermally and chemically stable, and does not tend to oxidize and corrode. However, the overall thermal and chemical robustness of a metal-coated carbon fiber contact might be ultimately limited by the coating metal. Also the carrier material, or other materials used in the assembly might be a limitation which has to be concerned.

7.2 Limitations

One reliability concern of the carbon fiber contact is broken fibers in the contact region. Short fiber fragments may serve as a contaminant to the contact interface and adversely impact interconnect or device reliability. Carbon fibers, especially the ones

exposed on the outside of the bundle, may break or fragment due to their fine size (i.e. 7-9 micron diameter) if sufficient shear force is applied.

Chapter 8 CONTRIBUTIONS

This dissertation presents a new inter-plane grid-array interconnect technique, which uses nickel-coated carbon fibers as the conductive medium. This is an innovative attempt to introduce carbon fiber into a new area in electronic applications.

To demonstrate the feasibility of the concept, a series of prototypes have been designed, fabricated and characterized. The characterization results based on these prototypes suggests that the new interconnect devices have their potentials in applications, in terms of multiple insertion cycles, electrical contact resistance, and self-inductance.

This dissertation initiates an exploration of nickel-coated carbon fibers' properties in a new application. Due to the limited prototypes characterized in this study, the observations and conclusions from this study are just “a tip of the iceberg”. As a first attempt, the results might not be comprehensive and accurate enough to be generalized to all types of carbon fiber electronic interconnects. There are still plenty of unknown areas to be discovered in the future study.

Chapter 9 SUGGESTIONS FOR FUTURE WORKS

9.1 Capacitance and mutual-inductance characterization

In the grid-array carbon fiber interconnect, the capacitance and mutual-inductance between contacts can be characterized, to evaluate the capacitive loss and cross-talk of signals transmitted in application.

9.2 Quantitative characterization of mechanical deflection

In Chapter 6, the mechanical deflection was qualitatively characterized. Factors including the fiber brush length, the number of fibers in bundle, the bundle diameter, the mechanical characteristics of the fiber and coating, and the smoothness of the pad can be considered in a quantitative characterization. A comprehensive understanding of the physics of the contact deflection is suggested, which is necessary to lead to the optimization of electrical and mechanical performance.

9.3 Reliability concern: breaking fibers

Carbon fibers are fragile, especially at the contact region. The breaking of carbon fibers could lead to performance and reliability problem, as discussed in the section of Limitation in Chapter 8: SUMMARY. Some approaches may be conducted to protect the fibers from breaking.

Appendices I – Examples of LGA sockets

Type	Manufacture / Product	Function	I/O capacity	Pitch (mm)	Descriptions
Bunched metal wire	Cinch wire fuzz button	Production	>1,000	1.00	Conductor: Au plated Mo wire
	HCD's SuperButton™	Production	>5,000	1.00	Conductor: Ni/Pd/flash Au plated Cu Alloy Carrier: FR4
Metal particle in elastomer	Tyco Electronics MPI	Production	24~5,000+	1.00, 1.27	Conductor: Ag particles embedded in elastomer Carrier: Polyimide
Metal Spring	Aries Sigma Spring	Test	256	1.00, 1.27, 1.50	Conductor: “ε” shaped Be-Cu
	InterCon Systems cLTA™	Production	<4,000	0.50, 1.00, 1.27	Conductor: “C” shaped Au/Ni plated Be-Cu
	Robinson-Nugent wire-in-elastomer	Production	N/A	N/A	Conductor: “S” shaped Be-Cu
	Adapters-Plus	Test & Production	20~1,000+	.80, 1.00, 1.27	Conductor: Au/Ni plated Brass alloy Carrier: Glass Epoxy FR-4
	Tyedyne MicroConn LGA Socket	Production	>2,500	1.00, 1.12, 1.27	Conductor: Au plated Be-Cu Carrier: Plastic matrix (LCP)
Other	Paricon Pariposer	Production	N/A	0.50, 0.65, 0.80, 1.00, 1.27	PariPoser Interconnects make electrical connections uniformly between opposing contact areas using BallWire conductive columns, which are regularly distributed within a sheet of silicone rubber

Appendices II - Related U.S. Patents of electronics connectors

U.S. Patent No.	Date	Inventor	Title
4,029,375	6/1977	Gabrielian	Miniature electrical connector
5,823,792	10/1998	Regnier	Wire-wrap connector
5,833,471	11/1998	Selna	Hold-down collar for attachment of IC substrates and elastomeric material to PCBS
6,033,233	3/2000	Haseyama et al	Electrical connecting device, and semiconductor device testing method
6,174,174	1/2001	Suzuki et al	Socket for IC and method for manufacturing IC
6,264,476	7/2004	Li,	Wire segment based interposer for high frequency electrical connection
6,695,623	2/2004	Brodsky et al	Enhanced electrical/mechanical connection for electronic devices
7,040,902	5/2006	Li	Electrical contact
2002/0106913	8/2002	Schuenemann et al	Continuous metal fiber brushes
2003/0049974	3/2003	Bauer et al	Electrical pressure contact
2003/0176083	9/2003	Li	Test and burn-in connector
2003/0207608	11/2003	Weiss	Very high bandwidth electrical interconnect
2004/0053519	3/2004	Li et al.	Coaxial elastomeric connector

References

- [1] H.O. Pierson, Handbook of Carbon, Graphite, Diamond and Fullerenes - Properties, Processing and Applications, William Andrew Publishing/Noyes, 1993
- [2] Tim. Pickford-Jones and Timmonet , “Joseph Swan”, Available at http://www.timmonet.co.uk/html/body_joseph_swan.htm, 2006
- [3] I.H. Shames and J.M. Pitarresi, Introduction to Solid Mechanics 3rd Edition, Prentice Hall, New Jersey, 2000, ISBN 0-13-267758-X, pp. 740
- [4] E. Thomson, “Carbon Brush”, United States Patent 539,454, May 21, 1895
- [5] Y. Wu, G. Zhang and W. Tang, “The research of fiber/graphite composite brush”, Electrical Contacts, 1995, pp. 315-322
- [6] S. Liu, “Carbon fiber contactor in polymer resistive position sensors”, Proceedings of the 47th IEEE Holm Conference on Electrical Contacts, IEEE, 2001, pp.282-287
- [7] R.F. Stinson, and J.A. Sarro, “The use of carbon fiber composites in sliding Contacts”, Proceedings of the 48th IEEE Holm Conference on Electrical Contacts, IEEE, 2002., pp.175-183
- [8] S.J. Wallace, J.E. Jedlicka and W.M. Peck (to Xerox Corporation), “Conductive brush paper position sensor”, U.S. Patent 4,641,949, February 10, 1987
- [9] S.J. Wallace, J.E. Courtney and W.M. Peck et al (to Xerox Corporation), “Switches and sensors utilizing pultrusion contacts,” U.S. Patent 5,420,465, May 30, 1995
- [10] W.S. Franks, J Randall and J.A. Swift (to Xerox Corporation), “Static eliminator”, United States Patent 4,553,191, November 12, 1985
- [11] J.A. Swift, T.E. Orłowski and S.J. Wallace et al (to Xerox Corporation), “Fibrillated pultruded electronic components and static eliminator devices,” U.S. Patent 5,354,607, October 11, 1994
- [12] J. Swift and S. Wallace, “Key aspects of the materials and processes associated with the synthesis and use of distributed filament contacts from PAN fiber based composites”, Proceedings of the 43rd IEEE Holm Conference on Electrical Contacts, IEEE, pp.190-200, 1997.
- [13] S.M. Lipka, “Electrochemical Capacitors Utilizing Low Surface Area Carbon Fiber”, IEEE AES Systems Magazine, July 1997, pp. 27-30
- [14] D.A. Shiffler, M.J. LaCour, et al, “Comparision of farbon fiber and cesium iodide-coated carbon fiber cathodes”, IEEE Transactions on Plasma Science, Vol. 28, No. 3, June 2000
- [15] H.D. Mansvelder, J.C. Lodder and K.S. Kits, “The use of the Van den Hul low noise carbon fibers in brain research”, 1998 H.D. Mansvelder, J.C. Lodder and K.S. Kits, 1998. <http://www.vandenhul.com/artpap/lsc-neuro.htm>

- [16] J.G. Partridge, S. Apparsundaram and G.A. Gerhardt et al, "Nicotinic acetylcholine receptors interact with dopamine in induction of striatal long-term depression", *The Journal of Neuroscience*, 22(7), April 1, 2002, pp. 2541-2549
- [17] D.D.L. Chung, "Electromagnetic interference shielding effectiveness of carbon materials," *Carbon*, Vol. 39, 2001, pp. 279-285
- [18] U. Kirbach, "The first metal free cable", *HiFi Exclusive*, 1993, available at <http://www.vandenhul.com/discontinued/frst-kirbach.htm>
- [19] M. Colloms, "The First interconnect and Revelation loudspeaker cable", *Stereophile*, Vol. 16, No. 3, pp. 134, May 1993, available at <http://www.vandenhul.com/artpap/mettle.htm>
- [20] A.J. van den Hul, "Carbon & Hybrid Technology", January 17, 1997, available at <http://www.vandenhul.com/artpap/hybrid.htm>
- [21] Steven R. Rochlin , "Avantgarde Acoustic Duo ", August 2005, available at <http://www.enjoythemusic.com/superioraudio/equipment/0705/avantgardeduo.htm>
- [22] Strother, *Physics*, Houghton Mifflin Company, Boston, 1977, ISBN: 0-395-21718-0, pp. 454
- [23] C.T. Ho, "Nickel- and copper-coated carbon fibre reinforced tin-lead alloy composites," *Journal of Materials Science*, Vol. 31, No. 21, November 1996, pp. 5781-5786
- [24] S.P. Shavkunov, M.I. Degtev, V.S. Korzanov, "A complex method of applying aluminum to carbon fiber", *Protection of Metals*, Vol. 39, No. 4, July 2003, 385-388
- [25] V. S. Dergunova, V.S. Kilin, A.V. Sharova, V.I. Frolov and A.P. Nabatnikov, "Carbon fibers coated with zirconium pyronitride," *Powder Metallurgy and Metal Ceramics*, Vol. 15, No. 6, June 1976, pp. 422 – 425
- [26] J. Xie, M. Pecht and et al., "An investigation of the contact behavior of electric distributed filament contacts", *IEEE Transactions on Components, Packaging, and Manufacturing Technology. Part A*, Vol.21, No.4, pp.604-609, December 1998
- [27] J. Xie, M. Pecht, A. Dasgupta, J. Swift and S. Wallace, "A statistical mechanical model of electrical carbon fiber contacts," *Transactions of the ASME the Journal of Electronic Packaging*, Vol. 121, December 1999, pp. 286-290
- [28] J. Xie, J. Hou, Y. Han, "A discussion of the contact behaviour of a carbon-fibre composite for electric contact applications," *Composites Science and Technology*, Vol. 59, 1999, pp. 1189-1194
- [29] J.S. Corbin, C.N. Ramirez and D.E. Massey, "Land grid array sockets for server applications", *IBM Journal of Research and Development*, Vol. 46, No. 6, November 2002
- [30] F.W. Grover, *Inductance Calculations Working Formulas and Tables*, Instruments Society of America, Dover Publications, June 1946, pp. 35
- [31] F.E. Terman, *Radio Engineers' Handbook*, McGraw-Hill, 1943

- [32] IPC and EIA associations STC and JEDEC, "IPC/EIA/JEDEC J-STD-002B: Solderability tests for component leads, terminals, lugs, terminals and wires", February 2003
- [33] Development of Sn-Zn Solder Paste of High Reliability, Showa Denko, IPC Works 1999
- [34] Cinch Connectors, "CIN::APSE specifications," available: http://www.cinch.com/view_sub_product_line.cinch?section_id=21§ion_title=CIN::APSE&sub_section_id=7411
- [35] High Connection Density, Inc., "Connector and socket product overview," April 2004, available: <http://www.hcdcorp.com/products/connectors/040408%20Connector%20Brief.pdf>
- [36] Tyco Electronics, "LGA application guide, Rev O" September 1, 2004, available: http://catalog.tycoelectronics.com/TE/Presentations/lga_appl.pdf
- [37] S. J. Wallace and J. A. Swift, "Fuzzy future for electronic contacts," EDN Products Edition, August 15, 1994, pp. 31-32
- [38] J.A. Swift and A.J. Werner (to Xerox Corporation), "Composite to enable contact electrostatic voltage sensing," U.S. Patent 5,220,481, July 15, 1993
- [39] J.A. Swift, T.E. Orlowski and A.J. Werner (to Xerox Corporation), "Pultruded conductive plastic connector and manufacturing method employing laser processing," U.S. Patent 5,250,756, October 5, 1993
- [40] T.E. Orlowski, J.A. Swift and S.J. Wallace et al (to Xerox Corporation), "Fibrillated pultruded electronic component," U.S. Patent 5,270,106, December 14, 1993
- [41] J.A. Swift and S.J. Wallace (to Xerox Corporation), "Multilayer wiring board interlevel connector, and method for making same," U.S. Patent 5,281,771, January 25, 1994
- [42] J.A. Swift, S.J. Wallace and J.E. Courtney et al (to Xerox Corporation), "Hollow pultruded electrical contact," U.S. Patent 5,410,386, April 25, 1995
- [43] J.A. Swift and S.J. Wallace (to Xerox Corporation), "High performance electric contacts," U.S. Patent 5,599,615, February 4, 1997
- [44] C.J. Bell, J.A. Vavonditte and F.R. Harmon et al (to Xerox Corporation), "Carbon fiber electrical contact for rotating elements," U.S. Patent 5,794,100, August 11, 1998
- [45] A.C. Larocca, J.W. Drawe and S.R. Hagell et al (to Xerox Corporation), "Carbon fiber electrical contact mounting for rotating elements", U.S. Patent 5,812,908, September 22, 1998
- [46] J.A. Swift, R.F. Ziolo and S.J. Wallace, "Electrical component containing magnetic particles," U.S. Patent 5,843,567, December 1, 1998
- [47] J.A. Swift (to Xerox Corporation), "Electrical component exhibiting clean laser cut," U.S. Patent 5,885,683, March 23, 1999

- [48] J.A. Swift (to Xerox Corporation), "Electrical component having fibers oriented in at least two directions," U.S. Patent 6,265,046 B1, July 24, 2001
- [49] J.A. Swift and J.R. Andrews (to Xerox Corporation), "Carbon fiber commutator brush for a toner developing device and method for making", U.S. Patent 6,289,187 B1, September 11, 2001
- [50] Bryte Technologies Inc., "Datasheet for EX-1510 resin system", available at <http://www.brytotech.com/webresources/pdf/ex-1510.pdf>, Accessed on May 2004